JPET Fast Forward. Published on March 10, 2005 as DOI: 10.1124/jpet.105.083428

Theta (θ) Isoform of PKC Alters Barrier Function in Intestinal Epithelium through Modulation of Distinct Claudin Isotypes: A Novel Mechanism for Regulation of Permeability.

A Banan, LJ Zhang, M Shaikh, JZ Fields, S Choudhary, CB Forsyth, A Farhadi, A Keshavarzian

Departments of Internal Medicine (Division of Digestive Diseases), Pharmacology, and Molecular Physiology, Rush University Medical Center, Chicago, IL 60612

Running Title: PKC-θ Modulates Claudins & Barrier Permeability

Address Correspondence to: A. Banan, Ph.D.

Associate Professor of Medicine, GI Physiology & Pharmacology

Director of Research, Gastroenterology & Nutrition

Rush University of Chicago, School of Medicine

Section of Gastroenterology and Nutrition

1725 W. Harrison, Suite 206

Chicago, IL 60612

Telephone Number: (312) 942-8973

Fax Number: (312) 563-3883

E-mail: ali_banan@rush.edu

Number of text pages: 22

Number of figures: 14

Number of Tables: 6

Number of references: 40

Number of Words in abstract: 249

Number of words in introduction: 743

Number of words in discussion: 1500

List of non-standard abbreviations: Wild type cells = [WT]; Sense expression of PKC-θ = [TRE-PKC-θ]; Anti-sense inhibition of PKC-θ = [AS-PKC-θ]; Dominant negative inhibition of PKC-θ = [Dominant neg. PKC-θ]; Inflammatory bowel disease = IBD.

JPET Fast Forward. Published on March 10, 2005 as DOI: 10.1124/jpet.105.083428
This article has not been copyedited and formatted. The final version may differ from this version.

ABSTRACT Using monolayers of intestinal Caco-2 cells, we discovered that the theta (θ) isoform of PKC, a member of the "novel" subfamily of PKC isoforms, is required for monolayer barrier function. However, the mechanisms underlying this novel effect remains largely unknown. Here, we sought to determine whether the mechanism by which PKC-θ disrupts monolayer permeability and dynamics in intestinal epithelium involves PKC-θ induced alterations in claudin isotypes. We utilized cell clones that we recently developed, clones which were transfected with varying levels of plasmid to either stably suppress *endogenous* PKC-θ activity (anti-sense, dominant negative constructs) or to ectopically express PKC-θ activity (sense constructs). We then determined barrier function; claudin isotype integrity; PKC-θ subcellular activity; claudin isotype subcellular pools; and claudin phosphorylation. Anti-sense transfection to under-express the PKC-θ led to monolayer *in*stability as shown by reduced**:** [1] *endogenous* PKC-θ activity, [2] claudin isotypes in the membrane & cytoskeletal pools (↓claud-1, ↓claud-4 assembly), [3] claudin isotypes phosphorylation (↓ phospho-serine, ↓ phospho-threonine), [4] architectural stability of the claudin-1 & claudin-4 rings, and [5] monolayer barrier function. In these anti-sense clones PKC-θ activity was also substantially reduced in the membrane & cytoskeletal cell fractions. In wild type (*WT*) cells, PKC-θ (82 kDa) was both constitutively active and co-associated with claudin-1 (22 kDa) and claudin-4 (25 kDa), forming endogenous PKC-θ/claudin complexes. In a 2nd series of studies, dominant negative inhibition of the endogenous PKC-θ caused similar *de*stabilizing effects on monolayer barrier dynamics, including claudin-1 & -4 hypo-phosphorylation, disassembly, and architectural instability as well as monolayer disruption. In a 3rd series of studies, sense over-expression of the PKC-θ caused not only a mostly cytosolic distribution of this isoform (i.e., <12% in the membrane + cytoskeletal fractions**,** indicating PKC-θ inactivity), but also led to disruption of claudins assembly and barrier function of the monolayer. **Conclusions**: PKC-θ activity is required for normal claudin assembly and the integrity of the intestinal epithelial barrier. These effects of PKC-θ are mediated at the molecular level by changes in phosphorylation, membrane assembly, and/or organization of the subunit components of two barrier function proteins: claudin-1 and claudin-4 isotypes. The ability of PKC-θ to alter the dynamics of permeability protein claudins is a new function not previously ascribed to the “novel” subfamily of PKC isoforms.

JPET Fast Forward. Published on March 10, 2005 as DOI: 10.1124/jpet.105.083428
This article has not been copyedited and formatted. The final version may differ from this version.

INTRODUCTION

The *epithelium* of the intestinal mucosa is the largest interface between the body and the external environment. An important characteristic of this interface is its ability to maintain a highly selective permeability barrier that protects the internal milieu from hostile factors in the lumenal environment. Barrier permeability, which in general is maintained by epithelial tight-junctional proteins, permits the absorption from the lumen of needed water and electrolytes, but prevents the passage of inflammatory and infectious agents (e.g., pathogenic bacteria) into the mucosa and systemic circulation. Loss of barrier function (i.e., increased permeability) is thought to lead to the penetration of bacterial derivatives and other harmful immunoreactive antigens into the mucosa and cause the initiation or perpetuation of inflammatory processes and tissue injury (Banan et al., 2000a; Hermiston and Gordon, 1995; Hollander, 1992; 1998; Keshavarzian et al.,1999). Indeed, disruption of barrier function ("leaky gut") has been implicated in the pathogenesis of several gastrointestinal and systemic disorders, including inflammatory bowel disease (IBD) (e.g., Hermiston and Gordon, 1995; Hollander, 1992; 1998; Keshavarzian et al., 1992; 1999; 2003; Peeters et al., 1994; Soderholm et al., 1999). Not surprisingly, one of the key difficulties in managing IBD patients stems from our incomplete understanding of the processes regulating intestinal barrier function.

A key discovery in recent years in IBD pathophysiology was the understanding that a leaky intestinal barrier, the so-called hyperpermeable-gut can lead to intestinal inflammation and tissue injury, and that maintaining a normal mucosal barrier function is required for intestinal health. For example, transgenic rodents with a hyperpermeable-intestinal-barrier exhibit intestinal mucosal inflammation (Hermiston and Gordon, 1995). Similarly, loss of intestinal barrier function induced by the injection of bacterial derivatives into the mucosa of rodents elicits IBD-like conditions (Yamada et al., 1993). Accordingly, investigating the molecular events underlying the alterations of gut barrier function is of fundamental biologic and clinical value.

In our efforts to better understand mechanisms underlying barrier disruption and gut inflammation, we have been investigating molecular mechanisms underlying loss of barrier function in the epithelium of the intestinal mucosa. Using monolayers of intestinal Caco-2 cells, as a well-established and widely used model for barrier function, we have reported (Banan et al., 1998b; 1999; 2000 a,b; 2001 a,b,c) that cytoskeletal assembly and stability is required for epithelial integrity. Moreover, we have shown that changes in Protein Kinase C (PKC) affect

epithelial barrier function (e.g., Banan et al., 2001 a,b). Although PKC, in general, is known to alter epithelial barrier, the role of specific PKC isoforms in barrier regulation and their mechanisms have remained largely unknown.

PKC consists of a family of serine and threonine-specific kinases, which includes at least 12 known isoenzymes that can be classified into three subfamilies (Banan et al., 2001 a,b; 2002a; 2003 a,b; 2004; Housey et al., 1988; Maruvada and Levine, 1999; Ponzoni et al.,1993). The conventional (or "*classical*") PKC isoforms (α, β1, β2, γ), the "*novel*" PKC isoenzymes (δ, ε, θ, η, μ), and the "*atypical*" PKC isoforms (λ, τ, ζ). Intestinal cells (including Caco-2 cells) express at least 10 isoforms of PKC, including PKC-α, PKC-β1, PKC-β2, PKC-δ, PKC-ε, PKC-θ, PKC-η, PKC-ζ, PKC-λ and PKC-τ (Banan et al., 2001 a,b; 2002 a; 2003a,b; 2004; Maruvada and Levine, 1999; McKenna et al., 1995). These isozymes differ in their mechanism of activation, subcellular distribution, substrate type, and expression, suggesting that each of these PKC isoforms can perform unique biological tasks (Banan et al., 2002a; 2003a; 2004; Melloni et al., 1990; Mischak et al., 1993; Person et al., 1988; Ponzoni et al., 1993). In our previous studies, we demonstrated both damaging and protective mechanisms/pathways affecting gut barrier integrity and permeability. For example, we showed that growth factors (EGF or TGF-α) prevent oxidant-induced barrier dysfunction via activation of the classical PKC-β1 isoform as well as by the atypical PKC-ζ (zeta) isoform, leading to monolayer protection (Banan et al., 2001b; 2003a,b). More recently, we reported novel findings that PKC isoform theta (PKC-θ) appears to affect epithelial barrier function (Banan et al., 2004). We showed that activation of the 82 kDa PKC-θ, a "novel" PKC isoform, is involved in epithelial barrier alterations. Despite the importance of the θ isoform of PKC to intestinal barrier permeability, the fundamental mechanisms underlying PKC-θ-mediated alterations in monolayer barrier function still remains largely unexplored.

The ability of the intestinal epithelium to maintain selective barrier permeability depends on a complex array of protein filaments which includes the cytoskeleton and barrier function proteins such as claudins (Banan et al., 1996; 1998a,b; 1999; 2000a,b; 2001b,c; Furuse et al., 1999; Unno et al., 1997; Yoo et al., 2003b). For example, claudins, a crucial family of barrier function proteins, constitute the major components of the junctional strands that delineate apical-lateral membranes as well as form the so-called seal (barrier) in the intercellular space (Fujibe et al.,

2004; Furuse et al., 1999; Ishizaki et al., 2003; Yoo et al., 2003b). The claudin family consists of at least 23 different isotypes that are essential in regulation of permeability function of cell monolayers (Furuse et al., 1999). In particular, claudin isotypes such as claudin-1 to -5 are thought not only to form aqueous pores within the cellular junctional strands, but also are important to paracellular permeability of the intestinal epithelium (Yoo et al., 2003b). The mechanisms underlying regulation of claudins and intestinal barrier function remain poorly understood.

In the current study, we determined the role of the θ (theta) isoform of PKC in the underlying mechanisms of barrier regulation and investigated possible alterations of key claudin proteins in regulation of the permeability of the intestinal epithelium. Exploring the role of the PKC-θ in the mechanism of epithelial barrier function is essential because**:** (1) it is of significant biological importance to establish the idea that "specific" isoforms of PKC play fundamental roles in endogenous modulatory mechanisms of cellular proteins required for the maintenance of intestinal barrier function; and (2) a better understanding of effectively modulating (e.g., by PKC-θ) the permeability function of the intestinal mucosal epithelium could lead to the development of novel therapeutic strategies for inflammatory diseases of the GI tract that are related to disruption of barrier function.

To this end, we studied the effects of PKC-θ on claudin proteins using three complementary molecular approaches. First, using an anti-sense approach, *native* (82 kDa) PKC-θ isoform was reliably under-expressed. Second, using a dominant negative approach, *endogenous* PKC-θ isoform was inactivated. Third, using a sense expression approach, *native* PKC-θ was reliably increased. We tested the *hypothesis* that PKC-θ isoform is required for changes in the dynamics of claudins assembly & cytoarchitecture and monolayer permeability function in intestinal epithelium. We now report novel mechanisms dependent on the PKC-θ isoform activity, namely alterations of the claudin-1 and claudin–4 isotypes phosphorylation, membrane assembly, and distribution as well as permeability function in cell monolayers. The biologic ability to change the dynamics of barrier function protein claudins is a new mechanism not previously attributed to the "novel" subfamily of PKC isoforms in cells.

MATERIALS AND METHODS

Cell culture. Caco-2 cells were obtained from ATCC (Rockville, MD) at passage 15. This widely used colonic cell line was chosen for our studies because they form monolayers that morphologically resemble intestinal cells, with defined apical brush borders and tight junctions, and a highly organized claudin-ring network upon differentiation (Banan et al., 1998; Gilbert et al., 1991; Meunier et al., 1995). Caco-2 cells are a transformed cell line and monolayers of tumor cells may respond differently than do non-transformed cells, including enterocytes in *native* tissue. Nonetheless, there is a wide body of evidence collected on these colonic cells over the last decade that shows their "normal" intestinal epithelial characteristics which makes them near ideal for gut barrier function studies. For example, Caco-2 cells form monolayers that can be studied for weeks, rather than just days, as is typical of most fresh *in vitro* preparations (Hurani et al., 1993; Meunier et al., 1995; Unno et al., 1997). This allowed us to measure alterations in intestinal barrier function. In addition, Caco-2 cells closely resemble *normal* intestinal cells in that they express intestinal hydrolases such as sucrase-isomaltase and alkaline phosphatase. Furthermore, these cells are similar to *native* intestinal epithelial cells in that they have receptors for prostaglandins, growth factors, VIP, LDL, insulin, and specific substrates such as dipeptides, fructose, glucose, hexoses, and vitamin B-12 (e.g., Banan et al., 1998; Gilbert et al., 1991; Meunier et al., 1995). Accordingly, this cell line provides a suitable *in vitro* model for our studies. To show the general validity of our findings, in select experiments another colonic cell line, namely HT-29 was utilized (Banan et al., 2002b; Balogh et al., 1995). Wild type cells or stably transfected cells (see below) were split at a ratio of 1:6 upon reaching confluency, and set up in either 6 or 24 well plates for experiments, or T-75 flasks for propagation. Cells were used 7-10 days post-confluence. The utility and characterization of these cell lines have been previously reported (Banan et al., 1996-2004; Balogh et al., 1995; Meunier et al.,1995).

Plasmids and Transfection. The sense, anti-sense and dominant negative plasmids of PKC-θ were constructed as we previously described (Banan et al., 2001b; 2002a; 2004). A unique tetracycline responsive expression (TRE) system was used to over-express the native PKC-θ. cDNA encoding the entire reading frame of PKC-θ plasmid was subcloned into the TRE vector creating TRE PKC-θ. The anti-sense or dominant negative PKC-θ plasmid was also subcloned to create AS-PKC-θ and dominant neg. PKC-θ.

Cultures of intestinal cells grown to 50-60% confluency were co-transfected with hygromycin resistance plasmid (pβ-hygro) and expression plasmids encoding either sense PKC-θ, anti-sense PKC-θ, or dominant negative PKC-θ by Lipofectin (Lipofectin reagent, GIBCO BRL) as we described (Banan et al., 2001b; 2004). Control conditions included vector alone. Briefly, cells were incubated for 16 h at 37 °C with the plasmid DNA in serum free media in the presence of lipofectamine (25 μl / 25 cm^2 flask). Subsequently, the DNA-containing solution was removed and replaced by fresh media containing 10% FBS to relieve cells from the shock of exposure to serum free media. Following transfection, cells were subjected to hygromycin selection (1 mg/mL). Resistant cells were maintained in DMEM / FBS and 0.2 mg/mL hygromycin (selection medium). For inducible expression of PKC-θ, cells were transfected with a plasmid expressing the tetracycline responsive transactivator **{**tTA**}** along with a second plasmid conferring resistance to G-418. After selection in 0**.**6 mg/mL of G-418 (selection media), one such clone (i.e., parental tTA) was then itself transfected with the TRE PKC-θ system. pβ-hygro was included to confer resistance to hygromycin (selection marker, 1 mg/mL). Control conditions included vector alone (TRE-z). Multiple clones expressing PKC-θ or lacking PKC-θ activity were assessed by immunoblotting and activity assay (Banan et al., 2004) and then used for experiments.

Experimental Design. In the <u>first</u> series of experiments, post-confluent monolayers of wild (naive) type cells were incubated with vehicle (isotonic saline) for 30 min and then assessed for base line conditions. Experiments were then repeated using multiple clones of stably transfected cells. In all experiments we assessed claudin skeletal stability (e.g., sub-apical ring cytoarchitecture), claudin subcellular distribution and assembly (claudin isotype distribution in membrane/cytoskeletal/cytosolic pools), claudin isotype phosphorylation (phospho-serine & phospho-threonine), PKC-θ intracellular distribution (membrane, cytoskeletal, cytosolic fractions), PKC-θ activity (immunoprecipitation & *in vitro* kinase assay), and monolayer barrier permeability (clearance of two different size fluorescent probes, FD70 kDa *versus* FD4 kDa).

In a <u>second</u> series of experiments, *sense* transfected cell clones over-expressing PKC-θ were utilized. To this end, multiple sense clones that were stably over-expressing PKC-θ (i.e., TRE PKC-θ) were grown as

monolayers and then exposed to vehicle. Outcomes measured were as described above. In these over-expression studies, cells were grown for 48 h in the absence of tetracycline before experiments.

In a third series of experiments, monolayers of *anti-sense* transfected cells lacking PKC-θ activity were treated with vehicle. In all experiments, PKC-θ activity was determined in immunoprecipitated samples (see below). In a corollary series of experiments, we investigated the effects of a PKC-θ *dominant negative* mutant on the state of monolayer barrier function, claudin isotype subcellular pool/assembly, and claudin isotype phosphorylation and cytoarchitecture. To this end, claudin isotypes (the structural protein subunit of permeability junctions) were isolated and then analyzed by immunoblotting. Claudin integrity was assessed by: (a) immunofluorescent labeling and fluorescence microscopy to determine the percentage of cells with normal claudin isotypes; (b) detailed analysis by high-resolution laser scanning confocal microscopy (LSCM); (c) immunoprecipitation and PAGE analysis of claudins.

Fractionation and Immunoblotting of PKC. Cell monolayers grown in large 75 cm^2 flasks were processed for the isolation of the cytosolic, membrane and cytoskeletal fractions as we described (Banan et al., 2001b; 2004). Protein content of these various fractions was assessed by the Bradford method (Bradford, 1976). Samples (5 μg protein/lane) were separated by PAGE. The immunoblotted proteins were visualized by enhanced chemiluminescence (ECL, Amersham, IL) and autoradiography (e.g., 1 h at -20 °C). The exposure times were adjusted to ensure linear responses. Under these conditions, the chemiluminescence assay was linear between 1 μg and 10 μg of total protein. Standard (purified PKC-θ) loading controls (1 μg/lane) were also run concurrently with each run. To further verify equal loading, blots were routinely stained with 0.1% India ink in TBST buffer.

For the isolation of the cell fractions, following treatments, post-confluent monolayers were scraped and ultrasonically homogenized (GE130, GE Ultrasonic Processor, amplitude 50, 6 pulses/sec, duration 20 sec) in Tris-HCl buffer **[**20 mM Tris-HCl (pH 7.5), 0.25 mM sucrose, 2 mM EDTA, 10 mM EGTA, aprotinin 2 μg/mL, pepstatin 2 μg/mL, leupeptin 2 μg/mL, and PMSF 2 μg/mL**]**. The homogenates were then ultra-centrifuged (100,000 g, for 40 min at 4° C) and the supernatant was removed and used as a source of the cytosolic fraction. Next, pellets were washed with 0.2 mL Tris-HCl buffer and resuspended in 0.8 mL buffer containing 0.3% triton X-100 and

maintained on ice for 1 h. The samples were then centrifuged (100,000 g, for 1 h at 4° C) and the supernatant was used as the source of the membrane fraction. To this remaining pellet we added 0.3 mL of cold (4° C) lysis buffer (150 mM NaCl, 50 mM Tris-HCl, 1 mM EDTA, 1 mM EGTA, 1% NP-40, 0.1% sodium deoxycholate, 0.1% SDS, aprotinin 2 μg/mL, pepstatin 2 μg/mL, leupeptin 2 μg/mL, and PMSF 2 μg/mL). The samples were then placed on ice for 1 h and ultra-centrifuged as above. The remainder of the lysate or triton-insoluble cytoskeletal fraction was then removed. For total extraction, which provides the fraction used to confirm total PKC-θ, scraped monolayers were placed directly into 1.5 mL of cold lysis buffer and subsequently ultra-centrifuged as described above. The supernatant was used for bulk protein determination.

For immunoblotting, samples (5 μg protein/lane) were added to a standard SDS buffer, boiled, and then separated on 7.5% SDS-PAGE (Banan et al., 2004). The immunoblotted proteins were incubated with a primary monoclonal antibody to PKC-θ **[**nPKC-θ (E7), #sc-1680 (human reactive), Santa Cruz Biotech, CA**]** at 1:3,000 dilution. A horse radish peroxidase-conjugated antibody (Molecular Probes, OR) was used as a secondary antibody at 1:4,000 dilution. Proteins were visualized by enhanced chemiluminescence and autoradiography, and subsequently analyzed by densitometry. The identity of the PKC-θ band was assessed by a procedure that we previously described (Banan et al., 2004)**:** 1) Using a PKC-θ blocking peptide (sc-1680 P, Santa Cruz Biotech) in combination with the anti-PKC-θ antibody that prevents the appearance of the corresponding "major" band in western blots. Additionally, 2) in the absence of the primary antibody to PKC-θ, no corresponding band for PKC-θ was observed. 3) The PKC-θ band ran at the expected molecular weight of 82 kDa as confirmed by a known positive control for PKC-θ (from rat brain lysates). 4) Pre-stained molecular weight markers (M_r 67,000 and 93,000) were run in adjacent lanes. In other studies using total PKC extracts, we confirmed our previous findings (Banan et al., 2004) that expression of PKC-θ or inhibition of PKC-θ did not affect the relative expression levels of other PKC isoforms.

Immunoprecipitation and PKC-θ Activity Assay. Immunoprecipitated PKC-θ was collected and processed for its ability to phosphorylate a synthetic peptide (Banan et al., 2004). Briefly, following treatments, confluent cell monolayers were lysed by incubation for 20 min in 500 μl of cold-lysis buffer **[**20 mM Tris-HCl, pH 7.4, 150 mM

NaCl, anti-protease cocktail (10 μg/ml), 10% glycerol, 1 mM sodium orthovanadate, 5 mM NaF, and 1% triton X-100**]**. The lysates were clarified by centrifugation at 14,000 g for 10 min at 4°C. For immunoprecipitation, the lysates were incubated for 90 min at 4°C with anti-PKC-θ (1:2,000 dilution, in excess). The extracts were then incubated with protein A/G plus agarose for 1 h at 4°C. The immunocomplexes were collected by centrifugation (2,500 g, 5 min) in a microfuge tube, washed 3 times with immunoprecipitation buffer containing 5 mM Tris-HCl, pH 7.4, and 0.2% triton X-100. They were then washed 1 time with kinase buffer (20 mM Hepes, pH 7.5, 10 mM $MgCl_2$, 2 mM $MnCl_2$, 20 μM ATP) and resuspended in 20 μL of kinase buffer and 5 μL of 5 X reaction buffer (1 mg/mL histone H1 and 0.25 mg/mL L-α-phophotidyl-L-serine) plus 5 μCi [γ-^{32}P]ATP and subsequently incubated for 5 min at 30°C. Reactions were then stopped by the addition of 8 μL of 5 X sample buffer, and the samples were boiled at 95°C for 5 min before separation by 7.5% PAGE. The extent of histone H1 phosphorylation was determined by scintillation counting of excised commassie-blue histone polypeptide bands. Counts for blanks were subtracted from the sample activity. Sample activity was also corrected for protein concentration (Bradford Method, Bradford, 1976), and PKC-θ activity was reported as pmol/min/mg protein.

Immunofluorescent Staining and High-Resolution Laser Scanning Confocal Microscopy of Claudin isotypes. Cell monolayers were fixed in a standard cytoskeletal stabilization buffer and then post-fixed in 95% ethanol at -20^{o}C as we described (Banan et al., 1998a,b; 1999; 2000a,b; 2001a,b,c). Cells were subsequently processed for incubation with an isotype specific primary antibody, monoclonal anti-claudin isotypes (claudin-1, -2, -3, -4, or -5; Zymed Labs, San Francisco, Ca), and then with a secondary antibody (FITC- and/or Texas Red-conjugated, Sigma). Following staining of claudins, cells were observed using a 63 X oil immersion plan-apochromat objective, NA 1.4 (Zeiss, Germany). The claudin elements were examined in a blinded fashion for their overall morphology, orientation, and disruption as we have described for other cytoskeletal components (Banan et al., 1998a,b; 1999; 2000a,b; 2001a,b,c). At least 1200 cells per group (200 X 6 slides) were examined by a blinded observer in four different sup-apical fields by laser scanning confocal microscopy and the percentage of cells displaying normal claudins was determined, reported as mean ± SEM. The identity of the treatment groups for all slides was decoded only after examination was complete.

In other studies, immunofluorescent analysis of the subcellular distribution of claudins was performed using monolayers that were 10 days post-confluence. Using laser scanning confocal microscopy, Z-scans of the entire height of cell monolayers were obtained with scans performed in 200 nm steps over a range of 10 μm (25-50 Z-stacks per cell monolayer area). Because claudins such as claudin-1 and claudin-4 exhibited the highest levels of expression at the "sub-apical" membrane (e.g., 1.8 μm sub-apical junctional) areas of intestinal cells, we focused on these areas in subsequent immunofluorescent studies.

Fractionation and Immunoblotting of Claudins. Subcellular fractions were isolated using the methods we described for fractionation and immunoblotting of PKC and cytoskeleton (e.g., Banan et al., 2003b; 2004). Following fractionation, the "claudin skeleton" was recovered by separately incubating (at 37°C for 30 min) the subcellular fractions (membrane, cytoskeletal, cytosolic) with stabilizing agents, 1 mM $MgSO_4$ and ATP (1 mM) in Cytoskeletal Stabilization Buffer (CSB) **[**0.1 M Pipes, pH 6.9, 30% glycerol, 5% DMSO, anti-protease cocktail (10 μg/mL), 1 mM EGTA, 1 mM $MgCl_2$, and 1 mM ATP**]**. Claudins were then recovered by centrifugation and resuspended in the above stabilization buffer (CSB). Fractionated samples were then flash frozen in liquid N_2 and stored at -70^{o}C until immunoblotting. For immunoblotting, samples (5 μg protein per lane) were placed in a standard SDS sample buffer, boiled, and then subjected to PAGE on 7.5% gels using appropriate (isotype specific) antibodies. Standard (purified) claudin loading controls (5 μg/lane) were run concurrently with each run. To additionally verify equal loading, blots were routinely stained with 0.1% India ink in TBST buffer. Furthermore, after the blots were stripped, actin (~43 kDa) immunoblotting was performed as an internal control for equal loading.

Analysis of Claudin Phosphorylation. Claudins were collected and assessed for phosphorylation by PAGE (Banan et al., 2004). For immunoprecipitation, cell lysates were incubated for 4 h at 4°C with isotype specific monoclonal anti-claudin antibodies (claudin-1, -2, -3, -4, or -5, 1:50 dilution, in excess). The extracts were then incubated with protein G plus Sepharose 4B (Zymed, San Francisco, CA) for 2 h at 4°C. The immunocomplexes were collected by centrifugation (2,500 g, 5 min) in a microfuge tube, washed 3 times with immunoprecipitation buffer containing 5 mM Tris-HCl, pH 7.4, and 0.2% triton X-100. The resultant pellets were resuspended in a standard SDS sample buffer, boiled at 95°C for 5 min before separation by PAGE. Gels were transferred to nitrocellulose membranes,

JPET Fast Forward. Published on March 10, 2005 as DOI: 10.1124/jpet.105.083428
This article has not been copyedited and formatted. The final version may differ from this version.

blocked with 1% bovine serum albumin and 0.01% Tween-20 in phosphate buffered saline for blotting by either anti-phosphoserine or anti-phosphothreonine (1:3,000 dilution; transduction Labs, Lexington, KY), and for detection of immune complexes by horse radish peroxidase-conjugated secondary antibody, and then incubated with chemiluminescent (ECL) reagents and autoradiographed.

To assess the specificity of claudin phosphorylation, in corollary experiments, blots used to detect the phosphoserine and phosphothreonine states of claudin immunoprecipitates were placed in protein stripping buffer and then reprobed with the corresponding isotype specific monoclonal claudin anti-bodies. These protocols were done to confirm that changes in the serine and threonine phosphorylation were in fact specifically associated with claudin-1 and claudin-4 proteins (and not due to simple reactivity against non-specific targets). To further assess phosphorylation specificity, we concurrently co-incubated the immunoprecipitated PKC-θ with the immunoprecipitated claudin (claudin-1 or -4) under *in vitro* (test tube) conditions. For these protocols, the PKC-θ immunocomplexes (1 mg/mL) were resuspended in 20 μL of kinase buffer (20 mM Hepes, pH 7.5, 10 mM $MgCl_2$, 2 mM $MnCl_2$, 20 μM ATP) and 5 μL of 5 X reaction buffer (containing 1 mg/mL claudin-1 or -4 and 0.25 mg/mL L-α-phophotidyl-L-serine) plus 5 μCi [γ-^{32}P]ATP and subsequently incubated for 5 min at 30°C. Reactions were then stopped by the addition of 8 μL of 5 X sample buffer, and the samples were boiled at 95°C for 5 min before separation by PAGE. Identical patterns of phosphorylation were seen as that of the protocols using immunoprecipitated claudins alone following PAGE.

In all experiments positive loading controls were run concurrently with each run. Specifically, for claudin phosphorylation blots, known positive controls (5 μg of corresponding phosphorylated claudins) were run with each gel **[**purified claudin isotype was phosphorylated by an *in vitro* kinase reaction via addition of 1 mg/mL PKC-θ in 20 μL of kinase buffer containing 20 mM Hepes, pH 7.5, 10 mM $MgCl_2$, 2 mM $MnCl_2$, and 20 μM ATP**]**. These positive controls also served as additional loading controls (5 μg of loading control per lane) that allowed for the comparison of data derived from different blots (or different days). Moreover, to ensure accuracy, loading controls were routinely run in duplicates or in some cases in triplicates. To further verify equal loading of lanes, blots were

routinely stained with 0.1% India ink in TBST buffer (containing 50 mM Tris-HCL, pH = 7.4, 150 mM NaCl, and 0.05% Tween-20).

Determination of monolayer barrier permeability by fluorometry. Status of monolayer barrier function was assessed by a widely used and validated technique that measures the apical to basolateral paracellular clearance of fluorescent markers such as fluorescein dextrans (FD70 kDa, 1 mg/mL) as we (e.g., Banan et al., 1999; 2000a,b; 20001a,b,c; 2002a) and others (e.g., Hurani et al., 1993; Sanders et al., 1995; Unno et al., 1997) described. In select experiments, a lower molecular weight fluorescein dextran (FD4 kDa, 1 mg/mL) was used. Briefly, fresh phenol free DMEM (800 μl) was placed into the lower (basolateral) chamber and phenol free DMEM (300 μl) containing probe (FD70 or FD4) was placed in the upper (apical) chamber. Aliquots (50 μl) were obtained from the upper and lower chambers at zero time and at subsequent time points and transferred into clear 96 well plates (Clear bottom, Costar, Cambridge, MA). Fluorescent signals from samples were quantitated using a Fluorescence multiplate reader (FL 600, BIO-TEK Instruments). The excitation and emission spectra for probes were: Excitation = 485 nm; Emission = 530 nm. In exploratory studies assessing barrier function in our PKC-θ transfected models, we consistently observed picomolar to nanomolar fluxes of FD in a range of sizes (4-70 kDa) across Caco-2 monolayers. Such FD flux was dependent on the transfected clones utilized (e.g., 1 μg anti-sense *versus* 5 μg anti-sense clone) and thus flux (clearance) increased with increasing amounts of DNA transfected. Also, when adding FD at concentrations in the range 0.001 to 1 mg/mL we observed a graded increase in FD flux. We were also able to consistently observe fluxes of picogram quantities of FD across monolayers. Clearance was then calculated as flux divided by surface area of the monolayer (Hurani et al., 1993; Sanders et al., 1995; Unno et al., 1997). Thus, Flux (nL/h) was calculated and subsequently normalized to surface area of monolayers (0.3 cm^2), and reported as a clearance (nL/h/cm^2). More specifically, Clearance (Cl) was calculated using the following formula: Cl (nL/h/cm^2) = Fab/([FD70 or FD4]a X S), where Fab is the apical to basolateral flux of FD70 or FD4 (light units/h, which is dependent on the fluorescent signals of samples obtained from the lower and upper chambers of transwell culture inserts), [FD70 or FD4]a is the concentration at base line (light units/nL), and S is the surface area (i.e., 0.3 cm^2). Simultaneous (concurrent) controls were run with each experiment.

Statistical Analysis. Data are presented as mean ± SEM. All experiments were carried out with a sample size of at least 6 observations per treatment group. Statistical analysis comparing treatment groups was performed using analysis of variance followed by Dunnett's multiple range test (Harter, 1960). Correlational analyses were done using the Pearson test for parametric analysis or, when applicable, the Spearman test for non-parametric analysis. *P* values < 0.05 were deemed statistically significant.

RESULTS

Our earlier findings (Banan et al., 2004) showed that intestinal cells co-transfected with complementary DNA (cDNA) encoding the hygromycin resistance (for selection) and the PKC-θ anti-sense (AS-PKC-θ) stably under-express the "novel θ" (82 kDa) isoform of PKC (*n*PKC-θ). Multiple clones of intestinal cells transfected with 1 to 5 μg of PKC-θ anti-sense cDNA demonstrated a dose-dependent under-expression of the PKC-θ *protein* (*Fig. 1A*, immunoblot). The clone transfected with 4 μg of PKC-θ anti-sense (-θ4) led to the largest reduction (~99%) in the levels of native PKC-θ protein while inducing maximum monolayer barrier disruption (increasing clearance of fluorescein sulfonic acid, FSA 0.478 kDa). Transfection of only the empty vector (control vector alone) did not do so. In the present investigation, we have studied the underlying mechanisms by which *n*PKC-θ affects barrier function.

Stable under-expression of the* n*PKC-θ isoform by anti-sense leads to instability of claudin isotypes assembly and architecture. Utilizing the aforementioned unique clones of intestinal Caco-2 cells, we first assessed the possible role of the PKC-θ isoform in the molecular dynamics of key claudin proteins involved in barrier function. Under-expression of *native* PKC-θ caused by transfection of anti-sense (AS-PKC-θ; 1, 2, 3, 4, or 5 μg cDNA) dose-dependently injured the claudin-1 ring-like skeleton *(Fig. 1A,* graph*)*. For example, for the 4 μg clone under-expressing PKC-θ (and exposed to vehicle) claudin-1 in the monolayer was disrupted as demonstrated by a *low* percentage of intestinal Caco-2 cells displaying the normal claudin-1 isotype. Indeed, the clone transfected with 4 μg of PKC-θ anti-sense (-θ4) provided maximum increases in claudin-1 instability. Wild type (WT) cells (those expressing *native* PKC-θ levels), in contrast, showed normal claudin-1 as demonstrated by high percentage of cells with intact claudin-1 isotype. As expected, transfection of only the empty vector by itself (vector alone) did not affect the claudin-1 isotype [% normal claudin-1 = 98 ± 2% for empty vector-transfected cells exposed to vehicle and 99 ± 1% for wild type cells exposed to vehicle]. In fact, both empty vector clones and wild type cells responded in a similar fashion to vehicle, exhibiting normal claudin-1.

Representative laser scanning confocal microscopy of immunofluorescently labeled claudin-1 corroborates *(Fig 1B, Panels a to c*) that the 4 μg clones under-expressing PKC-θ exhibited a loss of the normal claudin-1

skeletal-ring architecture (*Panel b, see arrows)*. This instability is seen in the intracellular appearance of a torn, beaded, and fragmented claudin-1 "ring" (from the "1.8 μm sub-apical" area of cell-cell contact). Wild type cells (*Panel a),* on the other hand, show an intact caludin-1 ring at these same areas of cell-cell contact. This normal architecture is indistinguishable from the *empty vector* transfected clones (*Panel c),* which were also exposed to vehicle.

We then assessed other claudin isotypes in our PKC-θ clones and native counterparts *(Figs 2A, 2B)*. *Native* PKC-θ under-expression in a dose-dependent fashion also injured the claudin-4 isotype ring-like skeleton *(Fig 2A).* As for claudin-1 isotype, the 4 μg PKC-θ anti-sense clone (-θ4) led to largest increases in claudin-4 isotype *in*stability. In wild type intestinal cells claudin-4 was normal. Furthermore, transfection of vector alone, as might be expected, did not affect the claudin-4 isotype [% normal claudin-4 = 100 ± 1% for empty vector-transfected cells exposed to vehicle and 100 ± 1% for wild type cells exposed to vehicle].

Laser confocal microscopy further revealed *(Fig 2B, Panels a to c)* that in wild type cells *(Panel a)* claudin-4 isotype, similar to claudin-1, appears as an intact ring on the inner side of the plasma membrane – i.e., "1.8 μm sub-apical" areas of cell-cell contact (*see arrows*). This is demonstrated by a continuous and smooth distribution of the claudin-4 ring-like architecture at these areas. Moreover, in PKC-θ under-expressing (4 μg) clones (*Panel b)* the claudin-4 ring shows a clear fragmentation and disorganization, whereas for the empty vector clone *(Panel c)* claudin-4 architecture was highly maintained (resembling wild type cells).

In comparison, other intestinal isotypes of claudin, including claudin-2, claudin-3 and claudin-5, did not appear to be affected by anti-sense to PKC-θ. For instance, representative "2 color" (double stain) studies of claudin-1 or -4 as compared, for example, to claudin-2 in the same intestinal cells (*Figs 3A, 3B*, respectively) showed that Caco-2 cells express little or no claudin-2 isotype (as compared to either claudin-1 or -4). Similarly, other representative "2 color" studies of claudin isotypes, including claudin-4 and claudin-2 (*Fig 3C*) corroborate the above findings. Studies of other claudin isotypes such as claudin-3 and claudin-5 are shown in *Fig 3D*.

Under-expression of endogenous* nPKC-θ *isoform causes a dynamic instability of monolayer barrier function: Increased permeability to Large Fluorescein Dextrans (FD70 kDa, FD4 kDa). Under-expression of *endogenous*

PKC-θ by anti-sense (AS-PKC-θ) led to loss of Caco-2 monolayer barrier function (*Table I.A).* In particular, barrier function in multiple clones of intestinal cells transfected with 1 to 5 μg of PKC-θ anti-sense plasmid showed a dose-dependent instability of monolayer permeability function as demonstrated by large increases in 70 kDa fluorescein dextran (FD70) clearance. Wild type (WT) cells (expressing *native* PKC-θ levels) showed normal permeability function. Interestingly, the clone transfected with 4 μg of PKC-θ anti-sense (-θ4) provided maximum increases in barrier permeability, paralleling findings on the instability of claudin isotypes -1 and -4. Transfection of the empty vector, as expected, did not disrupt barrier function [FD70 kDa Clearance = 0 ± 0 nL / h / cm^2 for vector-transfected cells exposed to vehicle and 0 ± 0 for wild type cells exposed to vehicle]. Both empty vector clone and wild type cells responded similarly to vehicle, showing normal barrier function.

Furthermore, there was also a dose-dependent instability of Caco-2 monolayer barrier function in the above noted AS-PKC-θ clones when we used a smaller size permeability probe, namely 4 kDa fluorescein dextran (FD4) *(Table I.A).* Not surprisingly, the 4 μg clone also exhibited maximum increases in monolayer permeability to FD4 kDa. Indeed, there was a size dependent increase in monolayer permeability in order of decreasing size for these probes (70 kDa FD < 4 kDa FD), suggesting the dynamic nature of barrier alterations. We observed a similar trend of alterations for disruption of both barrier function and claudin stability in another intestinal epithelial cell line, HT-29 (*Table I.B*). For example, 4 μg AS-PKC-θ clone also led to largest *in*stability in claudin (i.e., reduced % normal claudin-1 and claudin-4 isotypes) in HT-29 cells.

Because the clone transfected with 4 μg of AS-PKC-θ cDNA led to maximum levels of monolayer barrier disruption and claudins instability, we used this clone for subsequent mechanistic studies.

Anti-sense reduction of endogenous* n*PKC-θ leads to abnormal alterations in the membrane and cytoskeletal assembly of claudin isotypes. We determined the effects of *native* PKC-θ under-expression on the cytosolic, membrane and cytoskeletal pools of claudin-1 and -4 by assessing the 22 and 25 kDa (respectively) structural protein of these isotypes. The various subcellular claudin pools were isolated from the inhibitory (anti-sense) clones and analyzed following SDS-PAGE fractionation. *Tables II and III* show results of analysis for the subcellular distribution of claudin-1 and claudin-4 in the cytosolic, membrane, and cytoskeletal fractions of Caco-2 cells (data

presented as a fraction of total claudin isotype). These findings indicate that under-expression of PKC-θ abnormally decreases claudin-1 (*Table II*) and claudin-4 (*Table III*) in the membrane and cytoskeletal pools while concomitantly increases their proportions in cytosolic pools.

For example, PKC-θ under-expressing clone (4 μg AS-PKC-θ) exhibited an abnormal reduction in the particulate (particulate = membrane + cytoskeletal) pool of claudin-1 or claudin-4 as demonstrated by a decrease in its band density (*not shown*), indicating instability of claudin-1 or -4 assembly. In wild type cells, we did not find any decreases in the particulate pool of claudin, indicating normal assembly of claudin skeleton. In these wild type cells, as might be expected, claudin-1 or -4 particulate distribution was comparable to that found in the empty vector clone. Transfection of empty vector, as for its lack of effects on permeability and claudin architecture, had no affect on the particulate pool of claudin. These findings on the subcellular assembly/distribution of claudins parallel the *de*stabilizing effects of anti-sense, under-expression of *native* PKC-θ on intestinal claudins architecture and monolayer barrier function.

Anti-sense suppression of* n*PKC-θ causes alterations in serine- and threonine-phosphorylation states of claudin isotypes in intestinal epithelium. We subsequently probed molecular processes underlying the observed effects of PKC-θ on the monolayer claudins and barrier permeability. Accordingly, claudin-1 and claudin-4 isotypes were immunoprecipitated (by isotype specific antibodies) from the transfected and wild type cells, and subsequently subjected to PAGE to determine their phosphorylation *(Fig 4, A-D*). Immunoprecipitated claudin-1 isotype was largely serine and threonine phosphorylated in wild type cells *(Figs 4A, 4B*; corresponding *lane a*), but not in anti-sense transfected cells where suppression of *native* PKC-θ markedly decreased claudin-1 serine/threonine phosphorylation (corresponding *lane c*). We found a similar trend of alterations for the phosphorylation state of claudin-4 isotype in wild type and anti-sense clones *(Figs 4C, 4D).* In the empty vector clones both claudin isotypes were phosphorylated (corresponding *lane b in all blots*). The state of claudins serine/threonine phosphorylation in these vector clones resembled those of the wild type cells. When the same phosphorylation blots were stripped and reprobed with the corresponding isotype specific monoclonal claudin antibody, we confirmed that changes in phosphorylation were in fact specifically associated with the claudin-1 and -4 proteins (not shown).

Native* n*PKC-θ isoform is complexed with claudin. To further study the mechanism underlying the unique stabilizing affects of *native* PKC-θ on claudins, we used immunoprecipitation analysis *(Figs 5A-5D).* In a first series of approaches, cells were initially immunoprecipitated with a monoclonal PKC-θ antibody and then the immune complexes were analyzed for the presence of claudin-1, assessing whether this PKC isoform physically co-precipitates with claudin-1 isotype. Anti-sense clones under-expressing *endogenous* PKC-θ did not show any complex formation between these two proteins (*Fig 5A, lane c*). In contrast, transfection of the empty vector control did not do so, exhibiting co-precipitation of these two proteins (*lane d*). Similar to empty vector clone, the amount of claudin-1 co-precipitation was markedly enhanced in wild type (resting) vehicle treated cells (*lane b*), indicating likely presence of a PKC-θ /claudin-1 complex under *native* conditions. As expected, an irrelevant primary antibody (normal rabbit serum) did not lead to co-precipitation (i.e., no complex formation bands were seen), further suggesting specificity of the co-precipitation seen.

In a second (reverse) series of approaches (*Fig. 5B*), we further corroborated the aforementioned co-association findings. Here, anti-claudin-1 antibody was used and immunoprecipitates were then analyzed for the presence of PKC-θ. Not surprisingly, PKC-θ was not seen in the complex in anti-sense clones, i.e., no co-precipitation with claudin-1 *(lane c)*. On the other hand, wild type (vehicle) treated cells showed an accumulation of *native* claudin-1/PKC-θ complexes *(lane b)*, paralleling findings in figure 5A. Similarly, empty vector cells exhibited the formation of the endogenous claudin-1/PKC-θ complexes *(lane d)*. As before, an irrelevant antibody was ineffective (no co-precipitation).

In a third series of approaches, we further assessed the specificity of *inhibition* of formation of the PKC-θ/claudin-1 complexes in our PKC-θ anti-sense clones. Here, we probed lysates from two other PKC isoform anti-sense clones, the classical PKC-β2 and the PKC-α AS. As expected, in these other clones, we could not inhibit the formation of PKC-θ/claudin-1 complexes (not shown).

Using the aforementioned series of approaches, we found a similar trend of co-precipitation and complex formation between PKC-θ and claudin-4 isotype in intestinal cells *(Figs 5C, 5D).* As for claudin-1, probing lysates from other PKC isoform anti-sense clones - the classical PKC-β2 AS and the PKC-α AS - did not suppress the

formation of PKC-θ/claudin-4 complexes. This again indicates the specificity of PKC-θ/claudins co-precipitation we observed. Also, incubation with an irrelevant antibody was ineffective (not shown).

Subcellular activity and distribution of nPKC-θ: Native PKC-θ isoform is constitutively active and present mostly in the membrane & cytoskeletal fractions of intestinal cells. Findings from *in vitro* kinase activity assay of cytosolic, membrane, and cytoskeletal subcellular fractions (*Fig 6A*) confirm that the *native* θ isoform of PKC is mostly active in the particulate cell fractions (particulate = membrane and cytoskeletal fractions) with only a small activity in the cytosolic fractions, indicating the constitutive activity of the θ isoform of PKC under *native* conditions. Empty vector control was indistinguishable from the wild type cells. In anti-sense transfected clones under-expressing PKC-θ, on the other hand, there was an almost complete lack of *native* θ isoform activity as compared to the wild type cells. Immunoblotting assessment of the subcellular distribution of the PKC-θ protein (*Fig 6B*) additionally shows that the *native* (82 kDa) θ isoform of PKC is distributed mostly in the membrane and cytoskeletal fractions of wild type intestinal cells. Not surprisingly, in anti-sense clones, we found a near complete absence of PKC-θ protein in these same subcellular fractions, further indicating PKC-θ inactivity. Overall, these findings confirm that the endogenous PKC-θ isoform is "constitutively active" in the membrane and cytoskeletal (particulate) subcellular fractions because it is found to be most *active* in these fractions under *native* conditions. These findings on PKC-θ subcellular activity parallel our findings on the subcellular distribution and co-precipitation of claudin isotypes.

***Native* nPKC-θ activity robustly correlates with multiple indices of claudin isotype stability and barrier permeability function.** Using data across all-experimental conditions, we report significant ($p<0.05$) correlations ($r = 0.93, 0.95$, respectively) between PKC-θ activity (*in vitro* kinase activity assay from the membrane/cytoskeletal fractions) and enhanced monolayer claudin-1 and claudin-4 integrity/stability (i.e., % normal). We found other robust correlations when two other markers of monolayer barrier stability, either FD70 permeability (decreased FD 70kDa clearance) or FD4 permeability (decreased FD 4kDa clearance) were correlated with PKC-θ activity ($r = 0.96, 0.98$, respectively, $p<0.05$ for each). Additional robust correlations were found between other markers of monolayer barrier stability including enhanced claudin-1 or claudin-4 membrane/cytoskeletal pools (i.e., claudin-1 or claudin-4

assembly) and PKC-θ activity (r = 0.90, 0.92, respectively, $p<0.05$ for each). We found still other consistent correlations such as those between claudin-1 phosphorylation or claudin-1 stability and PKC-θ activation (r = 0.88, 0.97, respectively, $p<0.05$ for each) as well as between claudin-4 phosphorylation or claudin-4 stability and PKC-θ activation (r = 0.89, 0.94, respectively, $p<0.05$ for each).

Inactivation of endogenous nPKC-θ isoform in the membrane and cytoskeletal fractions by targeted dominant negative approach and its consequent destabilization of claudin membrane assembly and monolayer barrier function. The aforementioned findings together indicate that PKC-θ could play a pivotal intracellular function in claudin & barrier stability. We then further assessed the role of PKC-θ by utilizing an "independent" *dominant negative* approach to stably decrease the activity of endogenous PKC-θ isoform. Here, we used mutant clones we recently developed by transfecting cells with a PKC-θ dominant negative fragment and a plasmid encoding hygromycin resistance (Banan et al., 2004). Using this targeted approach, we are capable of markedly reducing the steady-state *activity* levels for *native* PKC-θ isoform in various subcellular fractions of these dominant negative mutants (*Fig 7*, 3 μg clone). In wild type cells, similar to empty vector clone, *native* PKC-θ isoform activity is high in the particulate (membrane and cytoskeletal) cell fractions, showing steady-state constitutive activity. As expected, dominant negative *fragment* transfection did not affect PKC-θ protein expression (not shown).

Table IV.A shows the dose-dependent effects of varying levels of PKC-θ dominant-negative plasmid (1-5 μg mutant cDNA) on Caco-2 monolayer barrier function assessed by FD70 clearance. We observed similar effects by PKC-θ dominant-negative plasmid in another intestinal cell line, HT-29 *(Table IV.B)*. Because transfection of 3 μg of dominant-negative plasmid to PKC-θ led to maximum barrier disruption (increased FD70 kDa clearance), this mutant clone was further utilized in subsequent studies.

Assessment of the percentage of mutant cells with a normal claudin-1 and claudin-4 architecture in Caco-2 monolayers demonstrates (*Figs 8A, 8B*, respectively*)* that dominant negative suppression of *endogenous* PKC-θ activity results in *in*stability of both claudin isotypes as demonstrated by *low* percentage (approximately 25%) of mutants displaying normal claudins. Claudin *in*stability was comparable to that seen in HT-29 mutant cells (*Table IV.B*). In wild type cells almost 100% of cells exhibit normal claudins.

Additionally, analysis of the subcellular distribution of claudin-1 (*Table II*) and claudin-4 (*Table III*) from the same mutant clones showed that dominant negative inactivation of *endogenous* PKC-θ largely leads to attenuation (reduction) of claudin isotypes in the membrane and cytoskeletal pools.

Representative immunoblot of the key particulate (membrane + cytoskeletal) pool from the same mutant clones corroborates that inactivation of PKC-θ reduces claudin isotypes in the particulate pool *(Fig 9*, claudin-1 shown*)*, indicating an abnormal claudin assembly.

Assessment of claudin phosphorylation from these mutant clones further demonstrates *(Figs 10A, 10B)* that inhibition of *native* PKC-θ activity markedly suppresses serine- and threonine- phosphorylation of claudin-1. Wild type cells show substantial, steady-state phosphorylation levels for claudin-1 isotype. Claudin-4 isotype followed an almost identical trend of changes in both wild type and dominant mutant cells (not shown).

Stable over-expression of nPKC-θ isoform protein in intestinal cells. The above findings using two independent molecular biological approaches (anti-sense, dominant negative) indicate that *native* PKC-θ plays a unique role in claudin and monolayer permeability alterations. Utilizing a third molecular approach, we further studied the role of PKC-θ in regulation of claudin assembly and barrier permeability by using intestinal cell clones that stably over-express the PKC-θ isoform (approximately 2 fold increase in 4 μg sense clones as compared to *parental* type cells) (*Fig. 11A, see immunoblot*). To this end, *parental* Caco-2 cells **{***tTA Parental***}** were co-transfected with plasmids encoding both hygromycin resistance and a tetracycline regulated expression (TRE) system for full-length *endogenous* PKC-θ, i.e., *TRE PKC-θ.* In this TRE system, over-expression (~2 fold elevation) of *native* PKC-θ is reached in the *absence* of tetracycline (TTX), whereas its presence decreases PKC-θ expression to the levels seen in the *parental* cell line. Utilizing such an approach, we investigated claudin isotypes and permeability alterations in both over-expressing and parental cell lines.

Over-expression of* n*PKC-θ isoform alters intestinal monolayer claudin assembly, phosphorylation, & cytoarchitecture and barrier permeability. *Table IV.A* depicts results of transfection experiments in Caco-2 cells that over-expression of PKC-θ [i.e., *TRE PKC-θ***]** by itself disrupts monolayer barrier function as demonstrated by increased FD70 probe clearance. Multiple clones of intestinal cells transfected with 1, 2, 3, 4 or 5 μg of *TRE PKC-*

θ plasmid show a dose-dependent increase in monolayer barrier permeability. HT-29 cells behaved in a similar manner, showing barrier disruption (*Table IV.B*). Transfection of only the empty vector (TRE-z) was ineffective (not shown). The clone transfected with 4 μg of *TRE PKC-*θ led to the highest increase in monolayer permeability and it was subsequently used for other experiments.

PKC-θ over-expression deleteriously affected monolayer claudins as demonstrated by low percentage of Caco-2 cells with normal claudins (*Figs 11A, 11B,* claudin-1*)*. As before, HT-29 cells behaved in a comparable manner (Table *IV.B*). This over-expression-induced *in*stability of claudin was suppressed when tetracycline was present (i.e., *TRE PKC-*θ + TTX). In *parental* cells, in contrast, claudin structure was normal, paralleling findings on barrier permeability. As before, transfection of the empty vector control was ineffective.

Laser confocal microscopy of the intracellular architecture of the monolayer claudin-1 (*Fig 11B, Panels a to d)* further corroborates that clones over-expressing PKC-θ (i.e., *TRE PKC-*θ exposed to vehicle) exhibit an abnormal rearrangement of the claudin-1 ring at areas of cell-cell contact (*Panel c).* This abnormality is shown by the appearance of a beaded, fragmented and disorganized claudin-1 ring (at the1.8 μm sub-apical cell-to-cell junctions). In the presence of tetracycline (which as noted prevents over-expression of *PKC-*θ*, Panel d)* these same clones exhibit a highly maintained and smooth claudin-1 ring. This normal architecture is indistinguishable from the *parental* cells exposed to vehicle (*Panels a & b*, with or without tetracycline, respectively*)*.

Changes in claudin-4 isotype architecture followed a similar pattern as demonstrated by confocal microscopy *(Fig 11C, Panels a to d)*. For example, in clones over-expressing PKC-θ (*Panel c, TRE PKC-*θ exposed to vehicle*)*, the claudin-4 isotype appears fragmented and disrupted. In the presence of tetracycline (*Panel d),* normal claudin-4 ring is seen. Similar to claudin-1, in *parental* cells (with or without tetracycline) *(Panels a and b,* respectively*)* claudin-4 ring architecture is intact.

Tables II and III show results of analysis for the subcellular distribution of claudin-1 and claudin-4 isotypes in the cytosolic, membrane and cytoskeletal fractions in clones over-expressing PKC-θ . In these TRE (over-expressing) PKC-θ cells both claudin-1 (*Table II*) and claudin-4 (*Table III*) were reduced in the membrane and cytoskeletal fractions (largely shifted into cytosolic fractions), further indicating claudin instability.

Representative immunoblot of the particulate pool *(Fig 12)* further corroborates that in cells over-expressing PKC-θ (*TRE PKC-θ* exposed to vehicle) the membrane + cytoskeletal pool of monolayer claudin-1 were markedly reduced (*lane c),* indicating an unstable claudin-1 assembly. Incubation of these clones with tetracycline (i.e., *TRE PKC-θ* + TTX, where tetracycline prevents over-expression of *PKC-θ*), as might be expected, maintained claudin-1 particulate pool at near normal. Similarly, *parental* type cells exposed to vehicle (with or without tetracycline) displayed a normal particulate pool of claudin-1. Transfection of the empty vector by itself was ineffective (i.e., both empty vector-transfected and *parental* cells responded in a similar fashion to vehicle, exhibiting a normal, steady-state claudin particulate pool). Changes in claudin-4 isotype membrane/cytoskeletal pool followed an almost identical trend (not shown).

Assessment of claudins phosphorylation further shows that PKC-θ ectopic expression also reduced claudins phosphorylation as determined by immunoblotting of immunoprecipitated claudin isotypes *(Figs 13A, 13B,* claudin-1 shown*)*. PKC-θ over-expressing cells show an abnormally low levels of serine and threonine phosphorylation for claudin-1 (see corresponding *lane c in both Panels*), which was prevented when tetracycline was present (corresponding *lane d*). In *parental* cells, claudin-1 serine/threonine phosphorylation was normal (*lanes a, b*). As expected, claudin-4 isotype phosphorylation followed a similar trend of alterations (not shown). The noted findings on barrier function claudin isotypes membrane assembly and cytoarchitecture as well as phosphorylation parallel the *de*stabilizing effects of PKC-θ over-expression on intestinal monolayer barrier permeability.

Over-expression of native* nPKC-θ *causes a reduction in the membrane and cytoskeletal associated activity of this isoform: PKC-θ activity correlates with several indices of monolayer claudin function. *Figure 14* shows results from *in vitro* kinase activity assay that over-expression of the PKC-θ (*TRE PKC-θ*) results in a substantial increase in the amount of its activity in the cytosolic fractions (while reducing membrane and cytoskeletal activities). When tetracycline is present, as expected, transfected clones {i.e., TRE PKC-θ + TTX} show near *native,* constitutive activity levels for PKC-θ in the membrane and cytoskeletal fractions. Moreover, *parental* cells exposed to vehicle (with or without tetracycline) {i.e., tTA parental ± TTX} show a normal steady-state, constitutive activity

for PKC-θ. This PKC isoform is constitutively active under these endogenous conditions because it is *natively* most active in the membrane and cytoskeletal cell fractions.

We now report other robust ($p<0.05$) correlations (e.g., $r = -0.94, -0.91$, respectively) such as between reduced PKC-θ activity (decreases in constitutive activity in the membrane/cytoskeletal fractions) and increased monolayer claudin-1 or claudin-4 isotypes *in*stability. When additional markers of monolayer barrier instability, reduced claudins particulate pool (e.g., decreased claudin-1 membrane assembly) or decreased claudin-1 serine/threonine phosphorylation or even increased barrier (FD) permeability were utilized against PKC-θ other robust correlations were found ($r = -0.92, -0.87, -0.90$, respectively, $p<0.05$ for each). Similar supporting correlations are reached when either monolayer barrier stability (e.g., FD70 permeability clearance) and claudins instability/disassembly (e.g., decreased claudin-1 membrane pool) were correlated ($r = -0.95$).

Collectively, these findings using targeted expression of PKC-θ (TRE PKC-θ) parallel our other findings on the *de*stabilizing effects of both PKC-θ under-expression (AS-PKC-θ) and PKC-θ inactivation (Dominant Neg. PKC-θ) on monolayer claudins and permeability function.

DISCUSSION

In the present investigation, we have demonstrated that the PKC-θ isoform is required for dynamic changes in claudin-1 and claudin-4 isotypes and for permeability function in the intestinal epithelium. The mechanism underlying this unique biologic effect of the -θ isoform of PKC appears to be alterations in the organization, assembly, and/or phosphorylation of the claudin isotypes. This is the first time that PKC-θ dependent mechanisms have been ascribed to the dynamics of permeability protein claudins in cells. We have thus discovered a novel biologic mechanism among the "novel" subfamily of PKC isoforms. These conclusions are based on several independent lines of evidence as discussed below.

First, anti-sense to native PKC-θ, which leads to under-expression of *endogenous* PKC-θ, induces *un*stable-like conditions to the monolayer claudins and barrier function. This *in*stability requires inactivation of the PKC-θ which is due to the decreased subcellular activity of this isoform in the critical membrane and cytoskeletal fractions. Second, suppression of PKC-θ by the same anti-sense causes *in*stability of the molecular dynamics of the barrier protein claudins. Here, inactivation of *native* PKC-θ (a) reduces both serine and threonine phosphorylation of claudins; (b) decreases the membrane/cytoskeletal distribution of claudins; (c) increases the instability of the molecular assembly of the claudins; and (d) reduces the percentage of intestinal cells displaying normal claudin-ring architecture. In contrast, in wild type cells the *native* (82 kDa) PKC-θ isoform is constitutively active in the key membrane and cytoskeletal pools as well as complexed with claudin isotypes. Third, dominant mutant inactivation of native PKC-θ causes an anti-sense-like *in*stability in the molecular dynamics of claudins and in permeability function in the intestinal epithelium. In these PKC-θ mutants, barrier dysfunction (i.e., increased permeability) was not only present, but also claudin isotypes exhibited decreased phosphorylation as well as reduced particulate levels and reduced cytoarchitectural integrity. Fourth, ectopic expression of native PKC-θ, which also induces a decrease in the subcellular activity of PKC-θ in the key membrane/cytoskeletal pools, evokes a sequence of *de*stabilizing alterations in these sense transfected clones. Indeed, in these sense clones, inducible expression of PKC-θ results in an almost identical and consistent cascade of disruptive changes to both cellular claudin isotypes and monolayer permeability. Collectively our findings strongly support a unique model for intestinal monolayer barrier dysfunction**:**

↓PKC-θ isoform activity ⇒ ↓claudin-1/claudin-4 isotype phosphorylation ⇒ ↑claudin-1/claudin-4 membrane/cytoskeletal pool instability (↓C1 and C4 isotypes assembly) ⇒ ↑claudin isotype ring architectural instability ⇒ ↑monolayer permeability.

In the current study, we mainly used Caco-2 cells because it has been extensively studied by us and is a reliable model for studying physiology (such as barrier function) and pathology (activation of inflammatory pathways), and the relevance of these findings to human diseases has been shown by several investigators (e.g., Banan et al., 1996-2004; Hurani et al., 1993; Keshavarzian et al., 1992; 2003; Meunier et al., 1995; Unno et al.,1997). More specifically, we and others have shown that monolayers of Caco-2 cells are a reliable and relevant model for (a) studying intestinal barrier function and (b) for evaluating mechanisms of barrier disruption (a key mechanism for IBD) and (c) for assessing efficacy and mechanisms of PKC modulation of barrier (a key goal of the current study) (e.g., Banan et al., 2000a,b; 2001a,b,c; 2002a; 2003a,b; 2004; Hurani et al.,1993; Keshavarzian et al., 1992; 2003; Meunier et al., 1995; Unno et al., 1997). We also showed that findings derived from this *in vitro* monolayer model are similar to those observed in *in vivo* studies such as those seen in tissues from patients with IBD (e.g., Keshavarzian et al., 1992; 2003). The similarities we previously reported between *in vitro* and *in vivo* results support the appropriateness of our Caco-2 model and its use for studying cellular and molecular mechanisms of barrier function/dysfunction.

Although PKC-mediated signal transduction is widely acknowledged to be important in epithelial cell function, its mechanisms have remained only poorly understood. In resting cells some PKC isoforms are inactive due to their predominant localization to cytosolic pools while other PKC isoforms are active due to their predominant localization to particulate (membrane and cytoskeletal) pools (Banan et al., 2003a; 2002a; Gopalakrishna and Jaken, 2000; Mullin et al., 1998). Different cell types not only express multiple isozymes of PKC, isozymes belonging to various subfamilies (classical, novel, atypical), but also, most PKC isotypes have unique modes of activation, substrate specificity, tissue expression, and subcellular distribution suggesting that each isoform of PKC mediates distinct biological functions (Babich et al., 1997; Banan et al., 2002a; 2003a,b; 2004; Housey et al., 1988; Melloni et al., 1990; Mischak et al., 1993). It is thus not surprising that the effects of PKC signaling in cells are highly complex and appear to vary widely with respect to experimental conditions as well as

tissue and cell types. For example, pharmacological studies suggest that PKC-ε, a member of "novel PKC subfamily", mediates cytokine-induced disruption of the intestinal cells (Yoo et al., 2003a). We previously showed that attenuation of the "*novel*" PKC isoform, PKC-δ, via molecular interventions protects against oxidant-induced damage to intestinal cells (Banan et al., 2002a). We also discovered that the 78 kDa "*classical*" -β1 isoform of PKC (PKC-β1) is key in protection of colonocytes against oxidant-induced injury (Banan et al., 2003b). Moreover, the 72 kDa "*atypical*" ζ (zeta) isoform of PKC (PKC-ζ) is also required for protection of colonocytes and acts by suppressing oxidative reactions, especially reactions mediated by iNOS and NO (Banan et al., 2003a). We have thus shown that both PKC-β1 and PKC-ζ isoforms perform unique tasks in mediating signaling cascades initiated by growth factors (EGF, TGF-α), which leads to <u>protection</u> of the intestinal epithelium (Banan et al., 2003a,b; 2004). Other PKC isoforms such as PKC-δ appear to have opposite effects, allowing or potentiating signaling processes induced by oxidants (H_20_2), which results in <u>injury</u> to the epithelium (Banan et al., 2002a). Thus, activating, inhibiting, or mimicking different isotypes of PKC leads to modification of distinct biological tasks and processes (e.g., protection, damage) in the intestinal epithelium. Our present findings on the 82 kDa PKC-θ, we believe, suggest a new function among the novel subfamily of PKC isoforms – "regulation" of epithelial barrier function through changes in phosphorylation, assembly and organization of the crucial claudin components of tight junctions.

Using monolayers of intestinal cells we reported (Banan et al., 1998b; 1999; 2000a,b; 2001a,b,c; 2003b) that tubulin and/or actin assembly is important to the maintenance of normal epithelial barrier permeability. A question that remains to be answered is: How do microtubule and/or even actin dynamics relate to claudins or other proteins involved in maintaining barrier function. Based on the known organization of tight-junctions, we propose a mechanism in which microtubules (tubulin) might affect barrier function proteins (claudins) and thereby affect barrier stability. In this view, tubulin, a known structural or adapter protein, is a critical regulatory protein linking cytoskeletal components (e.g., actin, microtubules) and tight-junctions (e.g., claudins, occludin, ZO). This mechanism requires that adapter proteins with a structural function exist and provide interactions between cytoskeletal components and barrier function proteins as was suggested by recent studies (e.g., Jin et al., 2002;

Tsukita et al., 2001). For example, ZO-1 (a protein localized to the tight-junction complex) is known to bind to claudins and occludin as well as to actin, and, more importantly, appears to function as an adapter (and as a structural protein) at the cytoplasmic surface of tight-junctions to stabilize or recruit other proteins, especially cytoskeletal proteins (Tsukita et al., 2001). Occludin (another barrier function protein) has a binding domain that binds to ZO, which in turn binds to the cytoskeleton. Indeed, such protein components form a huge macromolecular complex at the cytoplasmic surface of tight junctions where actin and microtubules are also found (e.g., inner side of sub-apical plasma membrane as we and others previously showed) (Banan et al., 1999; 2000a; 2003b). Thus, adapter proteins can act as critical regulatory and structural proteins, allowing interactions between barrier function (tight-junctional) proteins (e.g., claudins) and the cytoskeleton. Accordingly, loss of any key structural and/or adapter proteins (e.g., tubulin, actin, or ZO) may lead to breakdown of this macromolecular complex and the consequent injurious changes in epithelial barrier function. Consistent with this mechanism, we previously showed that stability of actin and microtubule cytoskeletons are critical to the maintenance of barrier function (e.g., Banan et al., 1999; 2000a,b; 2001a,b,c; 2003b). Not surprisingly, both microtubules and actin play a central role in maintaining cellular integrity, structure, and shape (e.g., Banan et al., 2000a; MacRae, 1992; Mandelkow and Mandelkow, 1995; Rodinov and Gelfand, 1993). As such, they also govern cell membrane morphology and polarity as well as intracellular transport, other functions essential to the maintenance of barrier function (e.g., Banan et al., 1998a; 2000a; Gilbert et al 1991).

Our series of reports on various PKC isoforms to date suggest a possible mechanism (target) for PKC isoform induced affects on intestinal barrier function – protein phosphorylation of cytoskeletal components through indirect or direct interaction (e.g., complex formation) with these proteins. For example, PKC-β1 over-expression causes an increase in serine phosphorylation of the tubulin subunits of microtubules while complexing with tubulin (Banan et al., 2001b; 2003b). This increase was prevented by anti-sense to PKC-β1 or when complex formation was suppressed. Similarly, in the current study, the θ isoform of PKC appears to complex with claudins and alter claudin phosphorylation (& barrier function) in intestinal cells, suggesting that this PKC isoform may be acting, directly or indirectly, on these tight junction proteins to alter barrier function. This mechanism is consistent with previous studies. PKC has been implicated in rearrangement of the cytoskeleton (e.g., Goodnight et al., 1995; Gopalakrishna and Jaken, 2000; Mischak et al., 1993; Person et al., 1988) and barrier function proteins (Yoo et al.,

2003a,b) although it is not completely known which PKC isoforms are key in these processes. Alternatively, PKC isoforms may target, directly or indirectly, phosphorylation of other tight junction proteins (e.g., ZO-1, ZO-2). Further studies will be needed to explore the nature of the interactions (complex formation) between PKC isoforms and their targets, especially tight junction proteins, in intestinal epithelial cells.

The ability of PKC-θ to affect the architectural organization and permeability of intestinal cells in monolayers could lead to development of new therapeutic modalities for a wide variety of intestinal disorders, especially IBD, where loss of mucosal permeability function has been found (Hermiston and Gordon, 1995; Hollander, 1992; 1998; Keshavarzian et al., 1992; 1999; 2003; Peeters et al., 1994; Soderholm et al., 1999). The pathophysiology of IBD, which includes ulcerative colitis and Crohn's disease, oscillates between active (symptomatic) phases of disorder when mucosal permeability is increased, and inactive (asymptomatic) phases when mucosal permeability is low. This waxing and waning in barrier permeability is consistent with the disrupted nature of barrier regulatory (structural proteins) in IBD mucosa. For example, we recently showed that the degree of mucosal structural protein instability (an index of barrier function) is closely correlated with the degree of inflammatory response and disease severity in IBD flare (Keshavarzian et al., 2003). The presence of unstable structural components, which indicates an abnormal, leaky gut barrier, has also been shown in intestinal epithelium under IBD-like conditions (Banan et al., 2000a; 2001b; 2002a; 2003a,b; 2004). These findings are further consistent with the current characterization of the pathophysiological development of IBD and its strong link to disruption of mucosal barrier function. For example, disruption of gut barrier permeability function elicits symptoms of inflammation and IBD-like responses in animals (Hermiston and Gordon, 1995; Yamada et al.,1993). Accordingly, a leaky gut is likely to be key in initiation and continuation of the IBD flare where mucosal inflammation leads to a vicious cycle of oxidative processes, barrier structural protein instability, and eventually mucosal injury. The regulatory effects of PKC-θ on barrier function, as we have observed in monolayers of intestinal epithelium, could be crucial in attenuating the perpetuation of barrier instability and inflammatory events in IBD. It is thus possible that changes in PKC-θ such as *in*activation (decreased expression) or even hyperactivation might occur during mucosal inflammatory states such as in IBD. Accordingly, up or down-

regulation of PKC-θ isoform activity could lead to barrier *in*stability seen in IBD. Future studies will be needed to explore this venue in IBD patients.

Although PKCs modulate almost all vital functions of cell, our knowledge of their mechanism is limited. This is mainly due to lack of potent and specific activators & inhibitors of PKC isoforms for assessing end points including barrier regulation. Pharmacological models, which currently are a major tool in investigation of these PKC isoforms depend mainly on "selectivity" of activators and inhibitors – a non-specific choice at best. Also, the very fact that PKC isoenzymes are involved in so many biological functions of cells makes it very hard if not impossible to isolate the desired pathway in the cells without interfering with others. Finally, compartment specific PKC isoforms (membrane or cytosolic) or sub-isotypes (e.g., -β1, -δ) might have different or even opposite functions, and this makes interpretation of experimental outcomes difficult. Fortunately, new techniques and agents especially "targeted molecular biology" are being developed (as we have done) and hold promise for helping to develop knowledge in this important area, especially to resolve issues concerning barrier function and disease processes.

REFERENCES

Babich M, Foti LR, and Mathias KL (1997) Protein kinase C modulator effects on parathyroid hormone-induced intracellular calcium and morphologic changes in UMR 106-H5 osteoblastic cells. *J Cell Biochem* 65(2): 276-285.

Banan A, Wang J-Y, McCormack SA, and Johnson LR (1996) Relationship between polyamines, cytoskeletal distribution, and gastric mucosal ulcer healing in rats. *Am J Physiol* 34(5): G893-G903.

Banan A, Smith GS, Rickenberg C, Kokoska ER, and Miller TA (1998a) Protection against ethanol injury by prostaglandins in a human intestinal cell line: role of microtubules. *Am J Physiol (GI & Liver)* 274 (37): G111-G121.

Banan A, McCormack SA, and Johnson LR (1998b) Polyamines are required for microtubule formation during mucosal ulcer healing. *Am J Physiol (GI & Liver)* 274(37): G879-G885.

Banan A, Choudhary S, Zhang Y, Fields JZ, and Keshavarzian A (1999) Ethanol-Induced Barrier Dysfunction and Its Prevention by Growth Factors in Human Intestinal Monolayers: Evidence for Oxidative and Cytoskeletal Mechanisms. *J Pharmacology & Experimental Therapeutics* 291(3):1075-1085.

Banan A, Choudhary S, Zhang Y, Fields JZ, and Keshavarzian A (2000a) Oxidant-induced Intestinal Barrier Function Disruption and Its Prevention by Growth Factors in a Human Colonic Cell Line: Role of the Microtubule Cytoskeleton. *Free Radical Biology & Medicine* 28(5): 727-738.

Banan A, Fields JZ, Zhang Y, and Keshavarzian A (2000b) Nitric Oxide and Its Metabolites Mediate Ethanol-Induced Microtubule Disruption and Intestinal Barrier Dysfunction. *J Pharmacology & Experimental Therapeutics* 294 (3), 997-1008

Banan A, Fields JZ, Zhang Y, and Keshavarzian A (2001a) Key Role of General Protein Kinase C Activation in EGF-Induced Protection of The Microtubule Cytoskeleton and Intestinal Epithelial Barrier Against Oxidant Injury. *Am J Physiol (GI & Liver)* 280: G828-G843.

Banan A, Fields JZ, Talmage DA, Zhang Y, and Keshavarzian A (2001b) The β1 Isoform of Protein Kinase C in EGF's Protection of Intestinal epithelium against Oxidant-induced Damage. *Am J Physiol (GI & Liver)* 281: G833-G847.

Banan A, Fields JZ, Zhang Y, and Keshavarzian A (2001c) Inhibition of Phospholipase C-γ Prevents EGF-Mediated Protection of The Microtubule Cytoskeleton and Intestinal Epithelial Barrier Function against Oxidant Injury. *Am J Physiol (GI & Liver)* 281: G412-G423.

Banan A, Fields JZ, Farhadi A, Talmage DA, Zhang L, and Keshavarzian A (2002a) Activation of the PKC-delta (δ) Isoform Is Required for Oxidant-Induced Disruption of Intestinal Epithelium. *J Pharmacology & Experimental Therapeutics* 303:17-28.

Banan A, Fields JZ, Talmage DA, Zhang L, and Keshavarzian A (2002b) The Atypical PKC-ζ Isoform Is Required for Protection of Microtubules and Intestinal Barrier Integrity. *Am J Physiol* **282**:G794-G808.

Banan A, Fields JZ, Zhang LJ, Shaikh M, Farhadi A, and Keshavarzian A (2003a) The Atypical Zeta (ζ) Isoform of Protein Kinase C Prevents Oxidant-Induced NF-κB Activation in The Intestinal Epithelium. *J Pharmacology & Experimental Therapeutics* 307:53-66.

Banan A, Zhang LJ, Shaikh M, Fields JZ, Farhadi A, and Keshavarzian A (2003b) Protein Kinase C-βeta1 Isoform Is Required for EGF-Induced NF-κB Inactivation and I-κBα Stabilization in Enterocyte Monolayers. *Am J Physiol* 286(3): C723-38.

Banan A, Zhang LJ, Fields JZ, Shaikh M, Farhadi A, and A. Keshavarzian (2004) Theta (θ) Isoform of PKC Is Required for Alterations in microtubule cytoskeletal Dynamics in Intestinal Epithelium: A Novel Function for PKC-θ. *Am J Physiol* 287(1): C218-34.

Balogh A, Csuka O, Tephan I, and Keri G (1995) Phosphatidylcholine could be the source of 1,2- diacylglycerol which activates protein kinase C in EGF stimulated colon cells (HT-29). *Cell Signaling* **7**: 793-801.

Bradford MA (1976) A rapid and sensitive method for the quantitation of microgram quantities of protein utilizing the principle of dye binding. *Anal Biochem* 72: 224-254.

Fujibe M, Chiba H, Kojima T, Soma T, Wada T, Yamashita T, and Sawada N (2004) Thr^{203} of claudin-1, a putative phosphorylation site for MAP Kinase, is required to promote barrier function of tight junctions. *Experimental Cell Research*, 295: 36-47.

Furuse M, Sasaki H, and Tsukita S (1999) Manner of interaction of heterogenous claudin species within and between tight junction strands. *J Cell Biology* 147:891-903.

Gilbert T, Le Bivic A, Quaroni A, and Rodreguez-Boulan E (1991) Microtubule organization and its involvement in the biogenic pathways of plasma membrane proteins in Caco-2 Intestinal epithelial cells. *J Cell Biol* 133(2):275-288.

Goodnight J, Mischak H, Kolch W, and Mushinski JF (1995) Immunocytochemical localization of eight PKC isoenzymes over-expressed in NIH 3T3 fibroblasts. *J Biol Chem* 270(17): 9991-10001.

Gopalakrishna R and Jaken S (2000) Protein Kinase C Signaling and Oxidative Stress. *Free Radical Biology & Medicine* 28(9): 1349-1361.

Harter JL (1960) Critical values for Dunnett's new multiple range test. *Biometrics* 16: 671-685.

Hermiston ML and Gordon JI (1995) Inflammatory bowel disease and adenomas in mice expressing a dominant negative N-cadherin. *Science* 270:1203-1207.

Hollander D (1992) The intestinal permeability barrier: A hypothesis as to its regulation and involvement in Crohn's disease. *Scand J Gastroenterol* 27:721-726.

Hollander D (1998) Crohn's disease- a permeability disorder of the tight junction? *Gut* 26, 1621-1624.

Housey GM, Johnson MD, Hsiao WLW, O'Brian CA, Murphy JP, Kirschmeier P, and Weinstein IB (1988) Overproduction of protein kinase C causes disordered growth control in rat fibroblasts. *Cell* 52:343-354.

Hurani MA and Noach AB, Blom-Roosemalen CM, DeBoer AG, Nagelkerke JF, Breimer DD (1993) Permeability enhancement in Caco-2 cell monolayers by sodium salicylate and sodium taurodihydrosulfate: Assessment of effect-reversibility and imaging of transepithelial transport routes by laser confocal microscopy. *J Pharmacology & Experimental Therapeutics* 267: 942-950.

Ishizaki T, Chiba H, Kojima T, Fujibe M, Soma T, Miyajima H, Nagasawa K, Wada I, and Sawada N (2003) Cyclic AMP induces phosphorylation of claudin-5 immunoprecipitates and expression of claudin-5 gene in blood-brain-

barrier endothelial cells via protein kinase A-dependent and -independent pathways. *Experimental Cell Research*, 290: 275-288.

Jin M, Barron E, He S, Ryan SJ, and Hinton D (2002) Regulation of Retinal Pigment Epithelial (RPE) intercellular junction integrity and function by Hepatocyte Growth Factor. *Investigative Ophthalmology and Visual Sciences*, 43(8): 2782-2790.

Keshavarzian A, Sedghi S, Kanofsky J, List T, Robinson C, Ibrahim C, and Winship D (1992) Excessive production of reactive oxygen metabolites by inflamed colon: Analysis by chemiluminescence probe. *Gastroenterology* 103:177-185.

Keshavarzian A, Holmes EW, Patel M, Iber F, and Pethkar S (1999) Leaky gut in alcoholic cirrhosis: a possible mechanism for alcohol induced liver damage. *Am J Gastroenterol* 94:200-207.

Keshavarzian A, Banan A, Kommandori S, Zhang Y, and Fields JZ (2003) Increased Colonic Free Radicals and Oxidative Injury to Key Cytoskeletal Proteins in Inflammatory Bowel Disease. *Gut* 52:720-728.

MacRae TH (1992) Towards an understanding of microtubule function and cell organization: an overview. *Biochem Cell Biol* 70: 835-841.

Mandelkow K and Mandelkow E (1995) Microtubules and microtubule-associated proteins. *Current Opinion Cell Biol.* 7:72-81.

Maruvada P and Levine AE (1999) Increased transforming growth factor-alpha levels in human colon carcinoma cell lines over-expressing protein kinase C. *International Journal of Cancer* 80(1):72-7.

McKenna JP, Williams JM, and Hanson PJ (1995) The alpha isoform of protein kinase C inhibits histamine-stimulated adenylate cyclase activity in a particulate fraction of the human gastric cancer cell line HGT-1. *Inflammation Research* 44(2): 66-69.

Melloni E, Pontremoli S, Sparatore B, Patrone M, Grossi F, Marks PA, and Rifkind RA (1990) Introduction of the ß isozyme of protein kinase C accelerates induced differentiation of murine erythroleukemia cells. *Proc Natl Acad Sci* USA 87:4417-4420.

Meunier VM, Bourrie Y, Berger Y, and Fabre G (1995) The Human Intestinal Epithelial Cell Line Caco-2: Pharmacological And Pharmacokinetics Applications. *Cell Biology & Toxicology* 11:187-194.

Mischak H, Goodnight J, Kolch W, Martiny-Baron G, Schaechtle C, Kazanietz MG, Blumberg PM, Pierce JH, and Mushinski JF (1993) Protein kinase C-α and -β in NIH 3T3 cells induce opposite effects on growth morphology, anchorage dependence, and tumorigenicity. *J Biol Chem* 268:6090-6096.

Mullin JM, Kampherstein JA, Laughlin KV, Clarkin CE, Miller RD, Szallasi Z, Kachar B, Soler AP, and Rosson D (1998) Protein kinase C-delta increases tight junction permeability in kidney LLC-PK1 cells. *Am J Physiol* 275(2 Pt 1):C544-54.

Persons DA, Wilkison WO, Bell RM, and Finn O (1988) Altered growth regulation and enhanced tumorigenicity of NIH 3T3 fibroblasts by protein kinase C. *Cell* 52:447-458.

Peeters M, Ghoos Y, and Maes B (1994) Increased permeability of macroscopically normal small bowel in Crohn's disease. *Dig Dis Sci* 39:2170-6.

Ponzoni M, Lacarelli E, Corrias MV, and Cornaglia-Ferraris P (1993) Protein kinase C isoenzymes in human neuroblasts: involvement of PKC-α in cell differentiation. *FEBS Lett* 322:120-124.

Rodinov VL and Gelfand VI (1993) Microtubule-dependent control of cell shape and pseudopodial activity is inhibited by the antibody to kinesin-motor domain. *J Cell Biol* 123: 1811-1820.

Sanders SE, Madara JL, Mcgurick DK, Gelman DS, and Colgan SP (1995) Assessment of inflammatory events in epithelial permeability: A rapid screening method using fluorescein dextrans. *Epithelial Cell Biol* 4: 25-34.

Soderholm JD, Peterson KH, and Olaison G (1999) Epithelial permeability to proteins in the non-inflamed ileum of Crohn's disease? *Gastroenterology* 117:65-72.

Soma T, Chiba H, Kato-Mori Y, Wada T, Yamashita T, Kojima T, and Sawada N (2004) Thr^{207} of claudin-5 is involved in size-selective loosening of the endothelial barrier by cyclic AMP. *Experimental Cell Research*, 300: 202-212.

Tsukita S, Furuse M, and Itoh M (2001) Multifunctional strands in tight junctions. *Nat Rev Mol Cell Biol*, 4:285-293.

Unno N, Menconi MJ, Smith M, and Fink MP (1997) Hyperpermeability of intestinal epithelial monolayers induced by NO: effect of low extracellular pH. *Am J Physiol* 272:G923-G934.

Yamada T, Sarto RB, Marshall S, Special RD, and Grisham MB (1993) Mucosal injury and inflammation in a model of chronic granulomatous colitis in rats. *Gastroenterology* 104:759-771.

Yoo J, Nicholas A, Song JC, Mammen J, Calvo I, Worrell RT, Cuppoletti J, Matlin K, and Matthews JB (2003a) Bryostatin-1 attenuates TNF-induced epithelial barrier dysfunction: role of PKC isozymes. *Am J Physiol* 284:G703-G712.

Yoo J, Nicholas A, Mammen J, Calvo I, Song JC, Worrell RT, Matlin K, and Matthews JB (2003b) Bryostatin-1 enhances barrier function in T-84 epithelia through PKC-dependent regulation of tight junction proteins. *Am J Physiol* 285:G300-G309.

Footnotes:

This work was supported in part by a grant from Rush University Medical Center, Department of Internal Medicine, and by three United States, National Institute of Health (NIH) grants (NIDDK 60511 and NCCAM 01581 to A. Banan; NIAAA 13745 to A. Keshavarzian). Address for reprint requests: Dr. A. Banan, Director of Research, Gastroenterology and Nutrition, Rush University Medical Center, 1725 W. Harrison, Suite 206, Chicago, IL 60612. E-mail: ali_banan@rush.edu

Portions of this work will be presented in the abstract form during the annual meeting of the American Gastroenterological Association (Digestive Disease Week), May 2005.

JPET Fast Forward. Published on March 10, 2005 as DOI: 10.1124/jpet.105.083428
This article has not been copyedited and formatted. The final version may differ from this version.

FIGURE LEGENDS

Figure 1A. Percent of intestinal Caco-2 cells with a normal claudin-1 isotype cytoarchitecture from multiple cell clones transfected with a plasmid encoding anti-sense to *native* PKC-θ (AS-PKC-θ). Uniquely transfected intestinal (Caco-2) cell clones we have recently developed that stably under-express the novel PKC-θ were utilized (*see immunoblot*). Note the dose-dependent under-expression of native PKC-θ protein (~82 kDa). PKC-θ anti-sense under-expression in a dose-dependent manner also deleteriously effects the claudin-1 skeleton as demonstrated by low percentage of cells with normal claudin-1 isotype **[**paralleling findings on monolayer barrier dysfunction (see Table I.A.)**]**. The 4 μg anti-sense clone, which effectively suppressed PKC-θ protein expression, led to the highest number of cells with unstable claudin-1. Wild type cells (those exhibiting native PKC-θ protein levels), on the other hand, show a high percentage of cells with stable (normal) claudin-1. Control empty vector clone, as might be expected, did not affect claudin-1. Cell monolayers were processed for immunofluorescent staining with a primary monoclonal anti-claudin-1 isotype antibody and subsequently the claudin-1 architecture was examined in a blinded fashion for its overall normal morphology. At least 1200 cells per group were examined in 4 different sub-apical fields by laser scanning confocal microscopy and the percentage of cells with normal claudin-1 was determined, reported as mean ± SEM. The identity of the treatment groups for all slides was decoded only after examination was complete. *p <0.05 *vs*. vehicle in wild type (WT) cells. +p <0.05 *vs*. vector alone transfected cells. (**WT**) = Wild type cells. (Vector alone) = Cells transfected with empty vector. AS-PKC-θ = Anti-sense inhibition of PKC-θ. N = 6 per group.

Figure 1B. Representative immunofluorescent photos showing the intracellular organization of the barrier function protein claudin-1 isotype (an index of monolayer integrity) in intestinal Caco-2 cells of wild type and transfected origin. Shown are images from both larger fields (top, *panels a-c*) and single cells (bottom, *panels a-c*). Intestinal monolayers grown on especially coated cover-slips were processed for staining and the claudin-1 isotype sub-apical organization was captured by high-resolution laser scanning confocal microscopy (LSCM). *Panel a* is from wild type monolayers exposed to vehicle. *Panel b* is from PKC-θ anti-sense (4 μg) clone exposed to vehicle.

JPET Fast Forward. Published on March 10, 2005 as DOI: 10.1124/jpet.105.083428
This article has not been copyedited and formatted. The final version may differ from this version.

Panel c is from empty vector clone exposed to vehicle. In wild type cells *(Panel a)* claudin-1 appears as an intact structure as shown by a smooth and continuous distribution of its "ring" at areas of cell-to-cell contact. Only in PKC-θ anti-sense clones (*Panel b)*, claudin-1 ring appears fragmented, beaded, and disorganized. In empty vector clones *(Panel c)*, as expected, claudin-1 organization is highly maintained and resembles normal (intact) morphology detected in that of wild type cells. Bar = 25 μm. Shown are representative photos. N = 6 per group.

Figure 2A. Anti-sense transfection against *native* PKC-θ isoform (AS-PKC-θ) induces a dose-dependent instability of monolayer claudin-4 isotype (another barrier function protein) in intestinal Caco-2 cells. Assessment of claudin-4 isotype in multiple PKC-θ anti-sense clones demonstrates a graded instability of claudin-4 as shown by reduced % of intestinal cells with normal claudin-4 isotype. The 4 μg anti-sense clone of PKC-θ, as for claudin-1 isotype, led to the maximum instability of claudin-4. Wild type (WT) cells, in contrast, exhibit a high percentage of cells with normal claudin-4 isotype. The empty vector clone (vector alone), as might be expected, did not affect claudin-4 stability. Intestinal monolayers were processed for staining with a primary monoclonal anti-claudin-4 isotype antibody and then examined in a blinded manner for claudin-4 normal morphology. *p <0.05 *vs*. vehicle in wild type (WT) cells. +p <0.05 *vs*. vector alone transfected cells. (**WT**) = Wild type cells. (Vector alone) = Cells transfected with empty vector. AS-PKC-θ = Anti-sense inhibition of PKC-θ. N = 6 per group.

Figure 2B. The architectural organization of the claudin-4 isotype (another index of monolayer integrity) as revealed by laser scanning confocal microscopy (LSCM) of Caco-2 monolayers of wild type and transfected origin. Shown are images from both larger fields (top, *panels a-c*) and single cells (bottom, *panels a-c*). *Panel a* is from wild type monolayers exposed to vehicle. *Panel b* is from PKC-θ anti-sense (4 μg) clone exposed to vehicle. *Panel c* is from empty vector clone exposed to vehicle. In wild type cells *(Panel a)* claudin-4 isotype is intact and smoothly distributed at sub-apical areas of cell-to-cell contact, whereas PKC-θ anti-sense clones *(Panel b)* exhibit clear disruption and instability of claudin-4 "ring". In empty vector clones *(Panel c)*, as expected, claudin-4 ring

architecture is highly maintained (intact), resembling the wild type cells. Bar = 25 μm. Shown are representative photos. N = 6 per group.

Figures 3A to 3D. The representative double stain ("2 color") studies of several claudin isotypes in intestinal Caco-2 cells of PKC-θ anti-sense transfected origin. *Figures 3A and 3B* show the representative 2 color studies of claudin-1 or -4 as compared to claudin-2 in the same intestinal cells. Other two color studies of claudin isotypes, including claudin-4 and claudin-2 (*Fig 3C*) and claudin-3 and claudin-5 (*Fig 3D*) are also shown. Colocalization ("yellow merge") is seen for all claudins, except for claudin-2 in Caco-2 cells (i.e., little or no claudin-2 is seen in Caco-2 cells, see 3B, 3C). Unlike the disrupted appearance of claudin-1 & -4 isotypes (see 3A), claudin-3 & -5 isotypes (see 3D) appear intact in PKC-θ anti-sense cells. Cells were processed for immunofluorescent staining with the corresponding FITC- and/or Texas red-conjugated primary antibodies. Shown are representative photos. N = 6 per group.

Figures 4A to 4D. Representative immunoblots of alterations in both serine- and threonine- phosphorylation states of immunoprecipitated claudin-1 *(Figs 4A, 4B)* and claudin-4 *(Figs 4C, 4D)* in intestinal Caco-2 cells of transfected origin as compared to wild type cells. Claudin isotypes were immunoprecipitated using the isotype specific monoclonal antibodies and subsequently immunoblotted to determine state of claudins phosphorylation. The bands representing claudin-1 and claudin-4 phospho-serine (*4A, 4C*, respectively) and claudin-1 and claudin-4 phospho-threonine (*4B, 4D*, respectively) correspond to: **[a]** wild type cells exposed to vehicle; **[b]** empty vector clone exposed to vehicle; **[c]** PKC-θ anti-sense clone (4 μg) exposed to vehicle. Anti-sense inhibition of endogenous PKC-θ isoform decreases claudins phosphorylation *(lane c)*, paralleling its *de*stabilizing effects on claudins subcellular assembly (*Tables II & III*) and claudins integrity (*Figs 1B, 2B*). These abnormally low phosphorylation levels are not seen in wild type cells (*lane a*) where claudin isotypes exhibit steady-state serine/threonine phosphorylation. Empty vector clone (*lane b*), as expected, did not affect phosphorylation (resembling the wild type cells). Shown are representative blots. N = 6 per group.

JPET Fast Forward. Published on March 10, 2005 as DOI: 10.1124/jpet.105.083428
This article has not been copyedited and formatted. The final version may differ from this version.

Figures 5A to 5D. PKC-θ anti-sense leads to a reduction in native co-association of the novel PKC-θ isoform and the barrier function protein claudin in intestinal Caco-2 cells – Claudin-1 isotype (*Figs 5A, 5B*) and Claudin-4 isotype (*Figs 5C, 5D*). Wild type cells show the endogenous PKC-θ /claudin complexes (see corresponding *lane b**, in 5A, 5B, 5C, 5D). Note the anti-sense inhibition induced reduction (disappearance) in co-immunoprecipitation of the PKC-θ / claudin complexes in transfected cells lacking PKC-θ isoform activity (*lane c*). For *figures 5A and 5C* immunoblots, cleared cell lysates were incubated with excess (1:2000 dilution) anti-PKC-θ bound to protein A beads and subsequently the immune complexes were resolved by PAGE utilizing the appropriate anti-PKC-θ or anti-claudin isotypes (claudin-1 or claudin-4) antibodies. Wild type (vehicle exposed) resting cells show endogenous PKC-θ /claudin complexes (see *lane b** in 5A, 5C). PKC-θ anti-sense clone displays no such endogenous PKC-θ/claudin complexes (*lane c*). For *figures 5B and 5D* blots opposite protocols were done in which the corresponding anti-claudin isotype antibody was used for immunoprecipitation and then the complexes formed were examined. As before, an almost identical pattern of complex formation (co-association) is seen between claudin/PKC-θ. The bands are from: **[a]** cell lysates; **[b]** wild type cells exposed to vehicle; **[c]** PKC-θ anti-sense clone (4 μg) exposed to vehicle; **[d]** empty vector clone exposed to vehicle. **WB** = western blot. **IP** = immunoprecipitated with the shown antibody. Shown are representative immunoblots. N = 6 per group.

Figures 6A and 6B. Assessment of PKC-θ activity (*6A*) and PKC-θ protein distribution (*6B)* in the subcellular fractions (i.e., cytosolic, membrane, cytoskeletal) of intestinal Caco-2 cells of anti-sense (AS) transfected and of wild type (native) origin. PKC-θ subcellular activity (by *in vitro* kinase assay) is shown in *Fig 6A.* PKC-θ subcellular protein distribution (by immunobloting) is shown in *Fig 6B.* Substantial activity/levels of the native PKC-θ isoform is seen in wild type cells. In these wild type cells most of the endogenous PKC-θ activity & protein is found in the particulate (i.e., membrane and cytoskeletal) fractions with a much smaller activity in the cytosolic fractions, indicating *native* activity of PKC-θ. Anti-sense inhibition of PKC-θ (4 μg AS-PKC-θ clone) almost completely inactivates the endogenous PKC-θ isoform (see *6A*). Also, note the almost complete absence of the

PKC-θ protein (see *6B*) in the same membrane, cytoskeletal, and cytosolic cell fractions. Cell monolayer extracts were immunoprecipitated by the anti-PKC-θ antibody and then processed for *in vitro* kinase assay to determine their ability to phosphorylate a synthetic peptide. Other extracts were processed for immunoblotting. *p <0.05 *vs.* wild type, *native* PKC-θ. +p <0.05 *vs*. vector alone transfected cells. Vector alone = Cells transfected with empty vector. AS-PKC-θ = Anti-sense inhibition of PKC-θ. Shown are representative blots. N = 6 per group.

Figure 7. D*ominant negative* inactivation of endogenous PKC-θ in intestinal Caco-2 cells transfected with a dominant negative plasmid for PKC-θ isoform. To suppress PKC-θ activity an independent approach involving a dominant negative fragment for the novel PKC-θ isoform was used. As before, subcellular extracts were subjected to immunoprecipitation and then processed for *in vitro* kinase activity assay. Note an almost complete inactivation of PKC-θ in the dominant negative mutants (3 μg clones). Wild type cells show the *native*, steady-state activity for PKC-θ in the membrane and cytoskeletal fractions. *p <0.05 *vs.* wild type, *native* PKC-θ. +p <0.05 *vs*. empty vector transfected clones. Empty vector = Cells transfected with only vector. Dominant neg. PKC-θ = Dominant negative inactivation of PKC-θ. N = 6 per group.

Figures 8A and 8B. Stable *dominant negative* inhibition of PKC-θ activity induces instability of both claudin-1 and claudin-4 isotypes in intestinal Caco-2 cells. A unique PKC-θ mutant cell line we have developed (see Methods) that near completely lacks *native* PKC-θ activity (see Fig 7) was utilized. In these dominant negative mutants, claudin-1 and claudin-4 are disrupted as shown by low percentage of mutant cells with normal claudins. In wild type cells nearly 100% of cells display normal claudin isotypes. *p <0.05 *vs.* vehicle in wild type (WT) cells. +p <0.05 *vs*. empty vector transfected cells. (**WT**) = Wild type cells. (Empty Vector) = Cells transfected with only vector. Dominant neg. PKC-θ = Dominant negative inactivation of PKC-θ. N = 6 per group.

Figure 9 Deleterious effects of the dominant negative inactivation of *native* PKC-θ on the assembly of representative claudin. In the mutant Caco-2 clone lacking PKC-θ activity normal assembly of claudin-1 is largely attenuated as shown by a reduction in band density of particulate (membrane + cytoskeletal) pool (*lane c*), paralleling findings on claudin-1 architectural *in*stability (8A, above). Either wild type cells or empty vector cells show normal (intact) assembly of claudin-1. The bands representing the particulate pools of claudin-1 are from: **[a]** wild type cells exposed to vehicle; **[b]** empty vector clone exposed to vehicle; **[c]** PKC-θ dominant negative (3 μg mutant) clone exposed to vehicle; **[d]** claudin standard (22 kDa, 5 μg/lane). Particulate (membrane + cytoskeletal) fractions were extracted from cells and ultimately processed for SDS-PAGE and x-ray film exposure. Shown is a representative immunoblot. N = 6 per group.

Figures 10A and 10B. Dominant negative inactivation of endogenous PKC-θ decreases claudin phosphorylation in Caco-2 cells. Representative claudin-1 isotype phosphorylation, phospho-serine and -threonine, in immunoprecipitated cell extracts from both mutant and wild type cells was examined. Cell extracts were immunoprecipitated by isotype specific monoclonal anti-claudin-1 before further processing by PAGE. The bands representing claudin-1 phospho-serine (10A) and claudin-1 phospho-threonine (10B) are from identical treatments as in figure 9. In wild type cells (*lane a*), claudin-1 exhibits normal, steady-state serine/threonine phosphorylation. However, in the dominant mutants (*lane c*) such phosphorylation is mostly attenuated. Shown are representative blots. N = 6 per group.

Figure 11A. *Over-expression* of PKC-θ isoform induces loss of claudin-1 integrity in transfected Caco-2 cells. We utilized clones transfected with a tetracycline responsive expression (TRE) system for PKC-θ [i.e., *TRE PKC-θ*]. In the *absence* of tetracycline/TTX, these clones over-express the *native* PKC-θ protein by 2.1 fold as compared to the parental cells (*see immunoblot*). Intestinal cells over-expressing PKC-θ [*TRE PKC-θ*] were incubated with or without tetracycline (TTX used to inhibit PKC-θ over-expression) or vehicle. Parental type [*tTA Parental*] cells (those expressing native levels of PKC-θ) were treated similarly. A low percentage of intestinal cells display normal

claudin-1 in the PKC-θ over-expressing cells. As might be expected, this injurious effect was inhibited in the presence of tetracycline in cell media [*TRE PKC-θ* + TTX]. Similarly, parental type [*tTA Parental*] monolayers exposed to vehicle (with or without tetracycline) show normal claudin as demonstrated a high percentage of cells with normal caludin-1. *p <0.05 *vs*. vehicle treated *Parental* cells. +p <0.05 *vs*. vehicle treated *TRE PKC-θ* cells incubated with tetracycline, "[*TRE PKC-θ* + TTX]". TTX = Tetracycline. [tTA Parental] = Parental cells. [TRE PKC-θ] = Cells transfected with tetracycline responsive expression (TRE) system for PKC-θ. For the immunoblot, pre-stained molecular weights M_r 67,000 and 93,000 were run in adjacent lanes. Shown is a representative blot. N = 6 per group.

Figure 11B. Representative fluorescent images showing the intracellular organization of claudin-1 isotype in Caco-2 cell clones as captured by high-resolution laser scanning confocal microscopy. Images shown are from both larger fields (*panels a-d*) and single cells (*panels a-d*). Monolayers of intestinal cells over-expressing PKC-θ were incubated with vehicle *(Panel c)* or vehicle plus tetracycline *(Panel d)*. In clones over-expressing PKC-θ (*Panel c*, TRE PKC-θ*)*, the claudin-1 "ring" is beaded, fragmented, and disrupted (see arrows). In the presence of tetracycline (which prevents PKC-θ over-expression, *Panel d)*, in this same clone normal claudin-1 architecture is maintained (intact). Similarly, in the *parental* cells with or without tetracycline *(Panels a and b*, respectively*)* claudin-1 ring appears intact at the sub-apical areas of cell-to-cell-contact. Bar = 25 μm. Shown are representative photos. N = 6 per group.

Figure 11C. The monolayer organization of claudin-4 isotype in Caco-2 cell clones assessed by high-resolution laser scanning confocal microscopy. Shown are images from both larger fields (*panels a-d*) and single cells (*panels a-d*). Intestinal cells over-expressing PKC-θ were incubated with vehicle *(Panel c)* or vehicle plus tetracycline *(Panel d)*. In clones over-expressing PKC-θ (*Panel c*, TRE PKC-θ*)*, the claudin-4 displays extensive disorganization, condensation, and beading of its sub-apical ring. In the presence of tetracycline (*Panel d)*, as for claudin-1 isotype, claudin-4 ring appears highly maintained. In the *parental* cells with or without tetracycline

JPET Fast Forward. Published on March 10, 2005 as DOI: 10.1124/jpet.105.083428
This article has not been copyedited and formatted. The final version may differ from this version.

(Panels a and b, respectively*)* claudin-4 isotype exhibits a normal ring pattern. The organization of claudin-4 in these *parental* cells is comparable to that of transfected clones with tetracycline (*Panel d)* (where tetracycline was used to inhibit PKC-θ over-expression). Bar = 25 μm. Shown are representative photos. N = 6 per group.

Figure 12. Immunoblot of the intracellular changes in the assembly of representative claudin isotype from the PKC-θ over-expressing clones and the parental type Caco-2 cells. Particulate (membrane + cytoskeletal) pool of claudin-1 isotype is largely reduced in PKC-θ over-expressing clones (*lane c*). Particulate pools were extracted from intestinal cells according to protocols we described before and processed for SDS-PAGE by monoclonal anti-claudin-1. The immunoblotted claudin-1 on nitrocellulose (NTC) membranes was then visualized by enhanced chemiluminescence (ECL) and autoradiography. The bands representing the intracellular assembly of claudin-1 from left to right are: **[a]** *Parental* type cells exposed to vehicle; **[b]** *Parental* type cells exposed to vehicle + tetracycline; **[c]** transfected PKC-θ over-expressing cells exposed to vehicle; **[d]** transfected PKC-θ expressing cells exposed to vehicle + tetracycline; **[e]** claudin-1 standard (22 kDa, 5 μg/lane). PKC-θ over-expression (*TRE PKC-θ)* disrupts dynamics of claudin-1 assembly (*lane c*). This disruption is seen in the reduction in particulate pool of claudin-1. In the same PKC-θ transfected clone, when tetracycline is present (*lane d*) normal claudin-1 assembly is maintained. This level of assembly now resembles that of the *parental* cells (*lanes a and b*). *Parental* cells show the normal, steady-state assembly of claudin-1 isotype. Shown is a representative blot. N = 6 per group.

Figures 13A and 13B. Representative alterations in the claudin serine/threonine phosphorylation in PKC-θ over-expressing clones as compared to parental type Caco-2 cells. Immunoprecipitated claudin-1 isotype was assessed for both serine and threonine phosphorylation. The bands representing claudin-1 phospho-serine (*13A*) and phospho-threonine (*13B*) correspond to: **[a]** *Parental* type cells exposed to vehicle; **[b]** *Parental* type cells exposed to vehicle + tetracycline; **[c]** transfected PKC-θ over-expressing cells exposed to vehicle; **[d]** transfected PKC-θ expressing cells exposed to vehicle + tetracycline. PKC-θ over-expressing clone displays a reduction in claudin-1 phospho-serine and phospho-threonine (corresponding *lane c*); this is largely attenuated by tetracycline

(corresponding *lane d*). Parental cells (with or without tetracycline) exhibit a normally phosphorylated claudin-1 isotype. Shown are representative blots. N = 6 per group.

Figure 14. *In vitro* kinase activity assay of the over-expressed PKC-θ in the cytosolic, membrane, and cytoskeletal subcellular fractions of intestinal Caco-2 cells. Over-expression of the PKC-θ (in TRE PKC-θ clone) leads to the distribution of most of its activity into the cytosol while reducing its membrane and cytoskeletal (i.e., particulate) activity. In contrast, parental cells exhibit *constitutive* activity of the native PKC-θ isoform in the membrane and cytoskeletal fractions (with little activity in the cytosol). As might be expected, in the presence of tetracycline PKC-θ transfected cells (i.e, *TRE PKC-θ* + TTX) display native constitutive activity of PKC-θ. *p <0.05 *vs.* corresponding vehicle treated *Parental* cells. +p <0.05 *vs*. corresponding vehicle treated *TRE PKC-θ* cells incubated with tetracycline, "[*TRE PKC-θ* + TTX]". TTX = Tetracycline. [tTA Parental] = Parental cells. [TRE PKC-θ] = Cells transfected with tetracycline responsive expression (TRE) system for PKC-θ. N = 6 per group.

Table IA. Effects of transfection of varying amounts of an anti-sense plasmid for the -theta (θ) isoform of PKC on intestinal Caco-2 monolayer barrier function

Treatment	FD *(70 kDa)* Clearance (nL/h/cm^2)	FD (*4 kDa*) Clearance (nL/h/cm^2)
Vehicle [WT]	0 ± 0	4 ± 3
Vehicle [Vector alone]	0 ± 0	6 ± 4
Vehicle [1 μg Anti-Sense PKC-θ DNA]	102 ± 15*+#	171 ± 28*+#
Vehicle [2 μg Anti-Sense PKC-θ DNA]	323 ± 21*+#	472 ± 30*+#
Vehicle [3 μg Anti-Sense PKC-θ DNA]	491± 18*+$^{\#}$	774 ± 25*+#
Vehicle [4 μg Anti-Sense PKC-θ DNA]	1201± 36*+	1678 ± 43*+
Vehicle [5 μg Anti-Sense PKC-θ DNA]	1189 ± 62*+	1646 ± 58*+

Cells were transfected with varying amounts of an anti-sense plasmid for PKC-θ (1, 2, 3, 4, or 5 μg DNA). The 4 μg anti-sense clone of PKC-θ displays the largest loss of monolayer barrier function. As expected, the empty vector alone did not affect monolayer barrier. Wild type (WT, un-transfected) monolayers are also shown. Monolayer barrier function was determined by clearance of two different size (70 kDa and 4 kDa) fluorescein dextran (FD) probes as described in methods. Values are means ± SEM. *$p < 0.05 vs.$ vehicle. +$p < 0.05 vs.$ vector alone clone. #$p < 0.05$ *vs.* cells transfected with 4 or 5 μg of anti-sense plasmid for PKC-θ. N = 6 per group.

Table IB. Effects of PKC-θ anti-sense on both monolayer barrier function and claudin integrity in another intestinal cell line, HT-29

Treatment	FD (*70 kDa*) Clearance (nL/h/cm^2)	% Normal Claudin-1	% Normal Claudin-4
Vehicle [WT]	0 ± 0	99 ± 1	100 ± 0
Vehicle [Vector alone]	0 ± 0	100 ± 0	100 ± 0
Vehicle [1 μg Anti-Sense PKC-θ DNA]	114 ± 11*+#	88 ± 2*+#	87 ± 3*+#
Vehicle [2 μg Anti-Sense PKC-θ DNA]	309 ± 16*+#	65 ± 4*+#	63 ± 5*+#
Vehicle [3 μg Anti-Sense PKC-θ DNA]	512 ± 19*+#	47 ± 3*+#	43 ± 2*+#
Vehicle [4 μg Anti-Sense PKC-θ DNA]	1257 ± 28*+	24 ± 5*+	21 ± 3*+
Vehicle [5 μg Anti-Sense PKC-θ DNA]	1210 ± 45*+	23 ± 3*+	19 ± 4*+

Human colonic HT-29 cells were transfected with an anti-sense plasmid for PKC-θ (1-5 μg). The 4 μg anti-sense clone causes the largest *in*stability of both claudin and barrier function. Wild type (WT) cells are also shown. Monolayer barrier function (clearance of fluorescein dextran, FD 70 kDa) and claudin integrity (% normal claudin isotype) were assessed as described in methods. Values are mean ± SEM. * $p < 0.05$ *vs.* vehicle. + $p < 0.05$ *vs.* vector alone clone. # $p < 0.05$ *vs.* cells transfected with 4 or 5 μg of PKC-θ anti-sense plasmid. N= 4-5 per group

Table II. Analysis of the subcellular distribution of Claudin-1 isoform in cell fractions from both transfected and wild type or parental intestinal cells

Treatment	Cytosolic Fraction	Membrane Fraction	Cytoskeletal Fraction
Native PKC-θ	5 ± 0.2	85 ± 2	10 ± 0.5
Empty Vector alone	5 ± 0.1	84. 5 ± 1	10. 5 ± 0.3
Anti-Sense PKC-θ	74 ± 4. 5*+	25 ± 2. 1*+	1. 0 ± 0.38*+
Dominant Neg. PKC-θ	72. 8 ± 5*+	26 ± 1.4*+	1. 2 ± 0.33*+
tTA Parental (native) PKC-θ	7 ± 1	81 ± 3.2	12 ± 0.61
tTA *Parental* + TTX	6. 6 ± 0.8	82 ± 4	11. 4 ± 0.7
TRE (over-expressing) PKC-θ	80 ± 6&#	18. 5 ± 3&#	1. 5 ± 0.4&#
TRE-PKC-θ + TTX	5 ± 2	83 ± 7	12 ± 0.39

Intestinal cells were transfected with either an anti-sense plasmid (4 μg) for PKC-θ or a dominant negative (3 μg) cDNA for this isoform. In corollary, other cells were transfected with a tetracycline regulated expression (TRE) system (4 μg) to over-express PKC-θ isoform. Cell monolayers were then treated with vehicle and/or where applicable tetracycline (TTX) and subsequently processed for the isolation of cytosolic, membrane and cytoskeletal cell fractions. Under native (or parental) conditions, claudin-1 is distributed mostly in membrane plus cytoskeletal (i.e., "particulate") cell fractions. In contrast, either *anti-sense* or *dominant neg.* PKC-θ clones show a mainly cytosolic pool of claudin-1 isoform, indicating its instability. In these cells, as might be expected, the particulate (membrane + cytoskeletal) pool of claudin-1 is reduced. Similarly, in *TRE (over-expressing)* PKC-θ cells claudin-1 is decreased in the membrane and cytoskeletal fractions (i.e., largely shifted into the cytosolic fractions), further indicating claudin-1 disruption. Relative subcellular levels of claudin-1 in various cell fractions were quantitated by measuring the anti-claudin-1 isoform immunoreactivity with a laser densitometer. Data reported as a fraction of total claudin-1. Total claudin-1 pool under the corresponding parental (native) or control condition was assigned an arbitrary value of 100 and all other pools were normalized to that value, reported in arbitrary units. Values are means ± SEM. *$p < 0.05$ *vs.* corresponding fraction of *native* (wild type) PKC-θ. +$p < 0.05$ *vs.* corresponding fraction of *empty vector* alone transfected cells. &$p < 0.05$ *vs.* corresponding *Parental* cells, i.e. "*tTA* Parental (native) PKC-θ ". #$p < 0.05$ *vs.* corresponding TRE-PKC-θ incubated with tetracycline, i.e. TRE-PKC-θ + TTX. N = 4 to 6 per group.

Table III. Subcellular distribution of Claudin-4 isotype from both transfected and wild type or parental intestinal cells

Treatment	Cytosolic Fraction	Membrane Fraction	Cytoskeletal Fraction
Native PKC-θ	8 ± 1	81 ± 3	11 ± 0.7
Empty Vector alone	7 ± 0.3	82 ± 4	11 ± 0.5
Anti-Sense PKC-θ	77 ± 6*+	22 ± 1.7*+	1.0 ± 0.22*+
Dominant Neg. PKC-θ	75 ± 3*+	23.5 ± 2*+	1.5 ± 0.1*+
tTA Parental (native) PKC-θ	7 ± 2	84 ± 5	9 ± 1
tTA *Parental* + TTX	6 ± 1	83 ± 6	11 ± 0.9
TRE (over-expressing) PKC-θ	81 ± 4&#	18 ± 2&#	1.0 ± 0.7&#
TRE-PKC-θ + TTX	6 ± 1.1	84 ± 5.5	10 ± 0.6

Intestinal cells were transfected with either anti-sense (4 μg) or dominant negative (3 μg) cDNA for PKC-θ isoform. Other cells were transfected with a tetracycline regulated expression (TRE) system (4 μg) to over-express PKC-θ isoform. Monolayers were treated with vehicle &/or tetracycline (TTX) and then processed for the isolation of cytosolic, membrane and cytoskeletal subcellular fractions. Under native (or parental) conditions, claudin-4 isotype is distributed mainly in membrane and cytoskeletal (i.e., "particulate") fractions. Either *anti-sense* or *dominant neg.* PKC-θ lead to a mostly cytosolic distribution of claudin-4 isotype. In these cells, the particulate (membrane + cytoskeletal) pool of claudin-4 is concomitantly decreased. In *TRE (over-expressing)* PKC-θ cells claudin-4 is also reduced in the particulate fractions (i.e., largely shifted out of the membrane and cytoskeletal fractions), indicating claudin-4 *de*stabilization. Relative levels of claudin-4 in subcellular fractions were quantitated by measuring the corresponding anti-claudin-4 isotype immunoreactivity with a laser densitometer. Data reported as a fraction of total claudin-4. Total claudin-4 pool under the corresponding parental (native) or control condition was assigned an arbitrary value of 100 and all other pools were normalized to that value, reported in arbitrary units. Values are means ± SEM. *$p < 0.05$ *vs.* corresponding fraction of *native* (wild type) PKC-θ. +$p < 0.05$ *vs.* corresponding fraction of *empty vector* alone transfected cells. &$p < 0.05$ *vs.* corresponding *Parental* cells, i.e. "*tTA* Parental (native) PKC-θ ". #$p < 0.05$ *vs.* corresponding TRE-PKC-θ incubated with tetracycline, i.e. TRE-PKC-θ + TTX. N = 4 to 6 per group.

Table IV.A. Effects of transfection of varying amounts of either a dominant negative or an inducible (tetracycline responsive expression) system/TRE for the PKC-theta (θ) on monolayer barrier function in Caco-2 cells

Treatment	FD *(70 kDa)* Clearance (nL/h/cm^2)
Vehicle [WT]	0 ± 0
Vehicle [1 μg Dominant Neg. PKC-θ DNA]	286 ± 17*#
Vehicle [2 μg Dominant Neg. PKC-θ DNA]	564 ± 24*#
Vehicle [3 μg Dominant Neg. PKC-θ DNA]	1255 ± 37*
Vehicle [4 μg Dominant Neg. PKC-θ DNA]	1288 ± 58*
Vehicle [5 μg Dominant Neg. PKC-θ DNA]	1179 ± 45*
Vehicle [Parental]	1 ± 1
Vehicle [Parental + TTX]	1 ± 1
Vehicle [1 μg TRE-PKC-θ DNA]	362 ± 18*#
Vehicle [1 μg TRE-PKC-θ DNA + TTX]	2 ± 2*
Vehicle [2 μg TRE-PKC-θ DNA]	893 ± 48*#
Vehicle [2 μg TRE-PKC-θ DNA + TTX]	4 ± 3*
Vehicle [3 μg TRE-PKC-θ DNA]	1869 ± 78*#
Vehicle [3 μg TRE-PKC-θ DNA + TTX]	5 ± 2*
Vehicle [4 μg TRE-PKC-θ DNA]	2247 ± 94*
Vehicle [4 μg TRE-PKC-θ DNA + TTX]	7 ± 7*
Vehicle [5 μg TRE-PKC-θ DNA]	2118 ± 114*
Vehicle [5 μg TRE-PKC-θ DNA + TTX]	11 ± 10*

Intestinal cells were transfected with a dominant negative plasmid for PKC-θ isoform (1, 2, 3, 4, or 5 μg DNA). In other experiments, cells were transfected with varying amounts (1, 2, 3, 4, or 5 μg DNA) of a tetracycline regulated expression (TRE) system to over-express PKC-θ. Wild type (WT) and/or parental monolayers are also shown. Monolayer barrier function was assessed by fluorescein dextran clearance as described in methods. Values are means ± SEM. *$p < 0.05$ *vs.* corresponding vehicle treated wild type or parental cells. #$p < 0.05$ *vs.* corresponding cells transfected with 4 or 5 μg of dominant negative-PKC-θ or TRE-PKC-θ. N = 6 per group.

Table IV.B. Effects of a dominant negative or an inducible (tetracycline regulated) system for PKC-θ on monolayer barrier function and claudin integrity in intestinal HT-29 cells

Treatment	FD (*70 kDa*) Clearance (nL/h/cm^2)	% Normal Claudin-1	% Normal Claudin-4
Vehicle [WT]	0 ± 0	100 ± 0	100 ± 0
Vehicle [1 μg Dominant Neg. PKC-θ DNA]	245 ± 21*#	77 ± 2 *#	76 ± 3*#
Vehicle [2 μg Dominant Neg. PKC-θ DNA]	592 ± 26*#	44 ± 5*#	41 ± 4*#
Vehicle [3 μg Dominant Neg. PKC-θ DNA]	1304 ± 51*	22 ± 3*	20 ± 2*
Vehicle [4 μg Dominant Neg. PKC-θ DNA]	1312 ± 43*	18 ± 2*	17 ± 5*
Vehicle [5 μg Dominant Neg. PKC-θ DNA]	1237 ± 39*	23 ± 4*	25 ± 3*
Vehicle [Parental]	0 ± 0	100 ± 0	99 ± 1
Vehicle [Parental + TTX]	0 ± 0	100 ± 0	100 ± 0
Vehicle [1 μg TRE-PKC-θ DNA]	299 ± 33*#	71 ± 3*#	69 ± 2*#
Vehicle [1 μg TRE-PKC-θ DNA + TTX]	5 ± 3*	95 ± 5*	96 ± 4*
Vehicle [2 μg TRE-PKC-θ DNA]	852 ± 57*#	37 ± 1*#	35 ± 2*#
Vehicle [2 μg TRE-PKC-θ DNA + TTX]	6 ± 5*	94 ± 4*	92 ± 7*
Vehicle [3 μg TRE-PKC-θ DNA]	1788 ± 59*#	14 ± 2*#	12 ± 1*#
Vehicle [3 μg TRE-PKC-θ DNA + TTX]	9 ± 3*	91 ± 5*	90 ± 6*
Vehicle [4 μg TRE-PKC-θ DNA]	2315 ± 76*	5 ± 3*	5 ± 2*
Vehicle [4 μg TRE-PKC-θ DNA + TTX]	10 ± 6*	87 ± 5*	88 ± 4*
Vehicle [5 μg TRE-PKC-θ DNA]	2234 ± 83*	8 ± 4*	7 ± 1*
Vehicle [5 μg TRE-PKC-θ DNA + TTX]	14 ± 8*	89 ± 5*	90 ± 3*

Human colonic HT-29 cells were transfected with either a dominant negative plasmid or a tetracycline regulated (TRE) system for PKC-θ (1-5 μg DNA). The 4 μg TRE-PKC-θ clone causes the maximum disruption of both barrier function and claudin; this is prevented when tetracycline (TTX) is present. Wild type (WT) cells and/or parental cells are also shown. Monolayer barrier function was assessed by clearance of fluorescein dextran (FD 70 kDa). Claudin integrity was assessed by % of cells with normal claudin. Values are mean ± SEM. * $p < 0.05$ *vs.* corresponding vehicle treated wild type or parental cells. # $p < 0.05$ *vs.* corresponding cells transfected with 4 or 5 μg of dominant negative PKC-θ or TRE-PKC-θ plasmid. N= 4 per group.

Figure 1A.

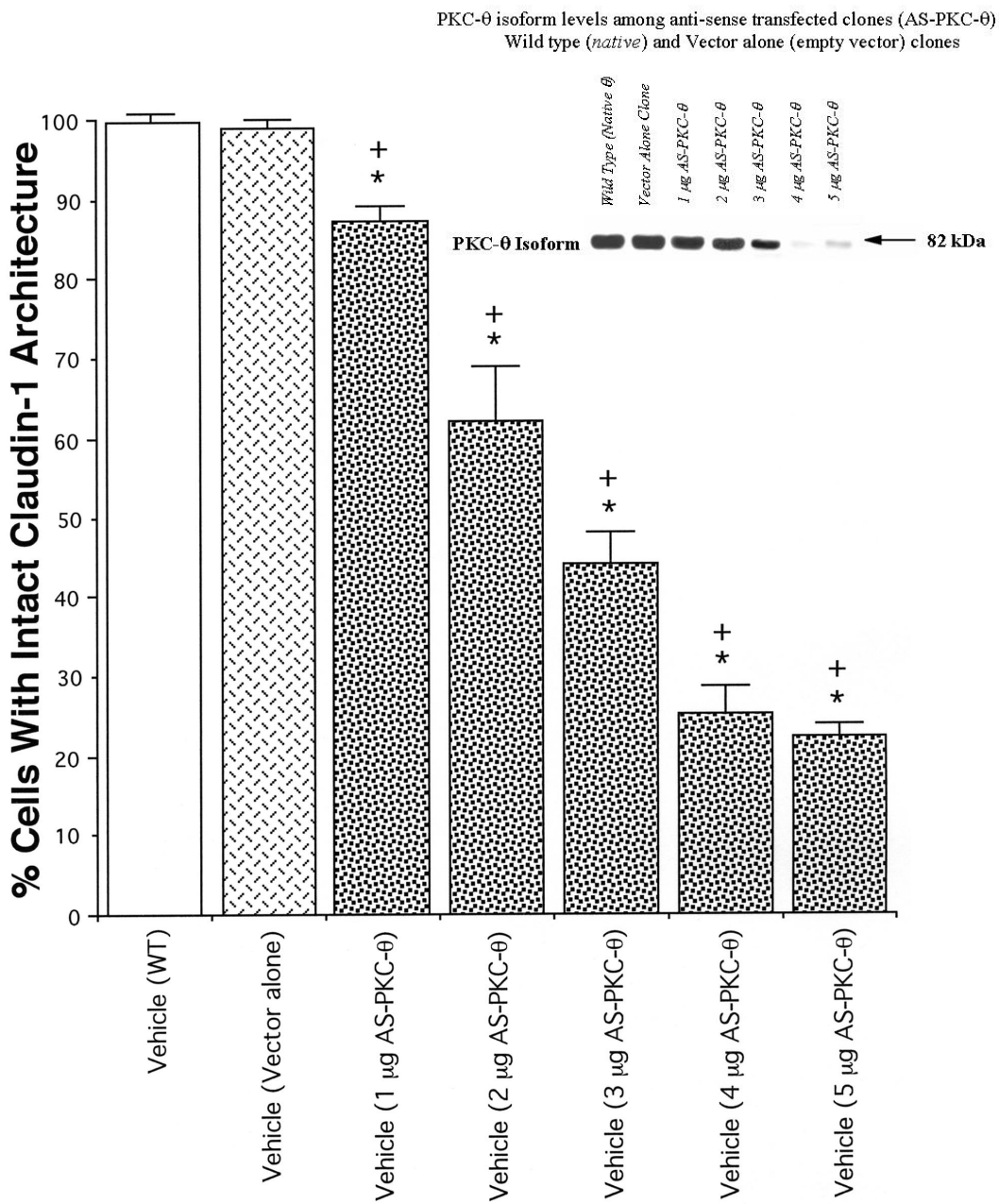

Figure 1B. **Representative Images of Claudin-1 Isotype Architecture In Monolayers**

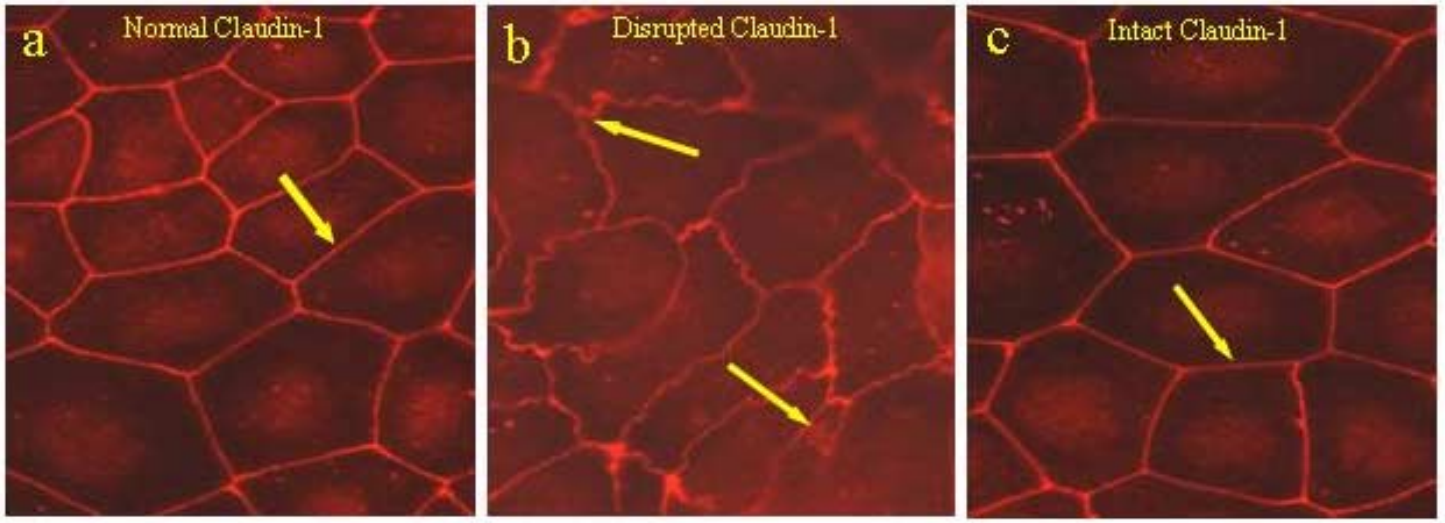

Claudin-1 Architectural Details in Single Cells of Anti-sense and Wild Type Origin

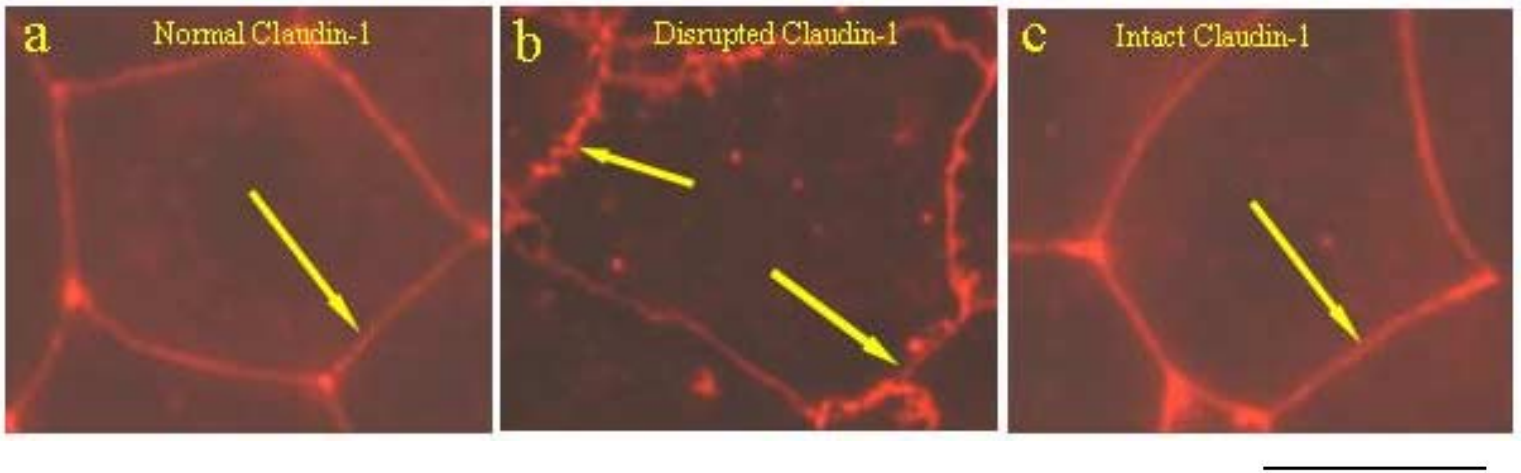

JPET Fast Forward. Published on March 10, 2005 as DOI: 10.1124/jpet.105.083428
This article has not been copyedited and formatted. The final version may differ from this version.

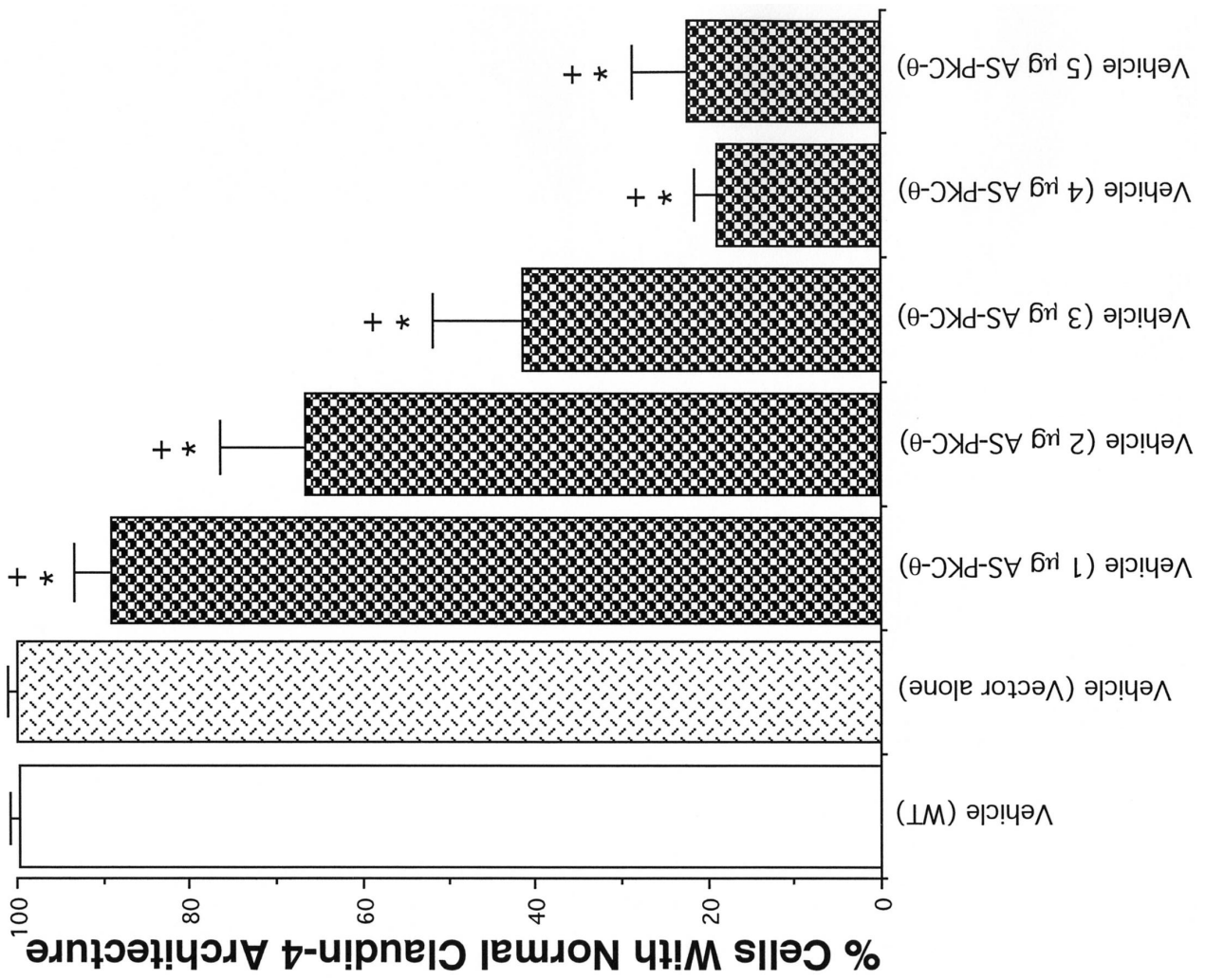

Figure 2A.

Figure 2B.

Representative Claudin-4 Isotype Cytoarchitecture in Monolayers

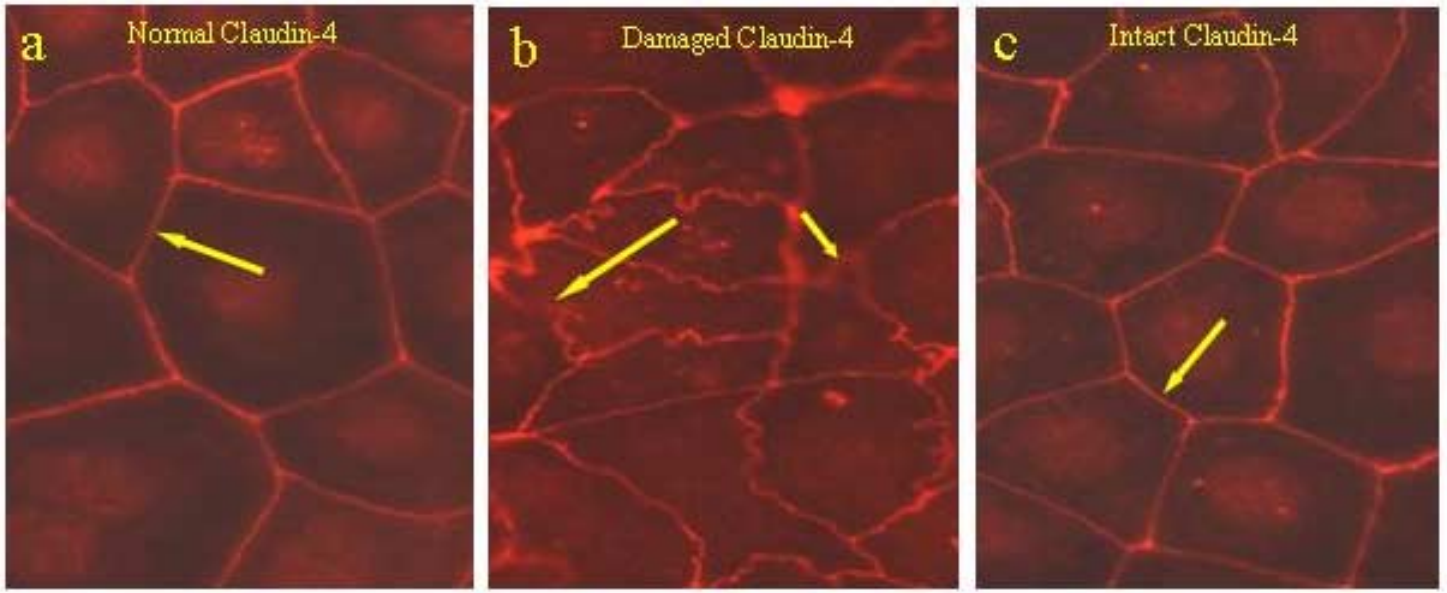

Claudin-4 Architectural Details in Single Cells of Anti-sense & Wild Type Origin

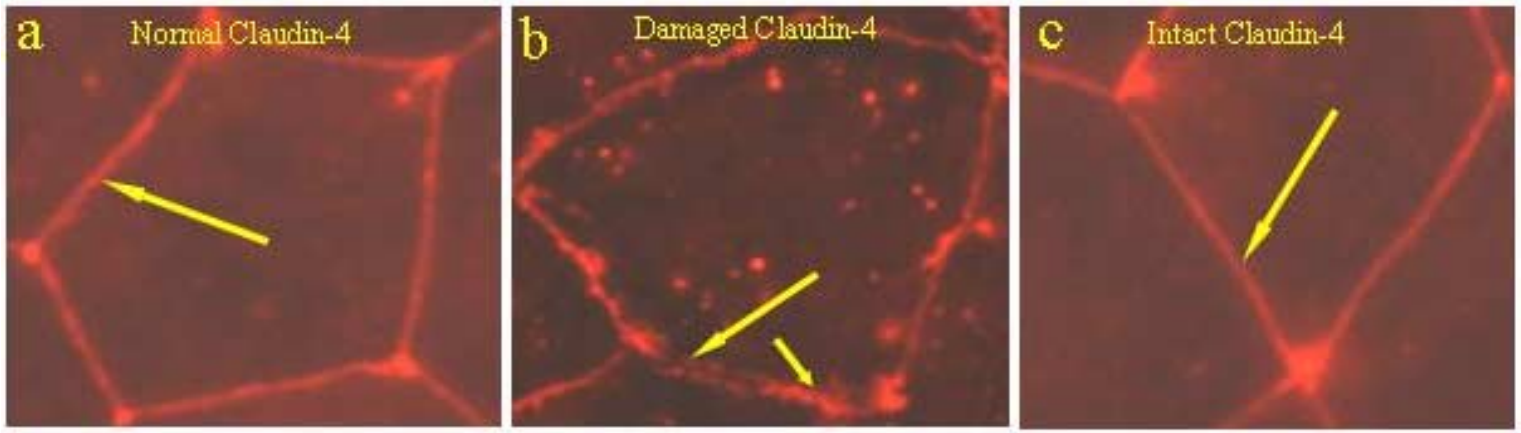

Figures 3A to 3D.

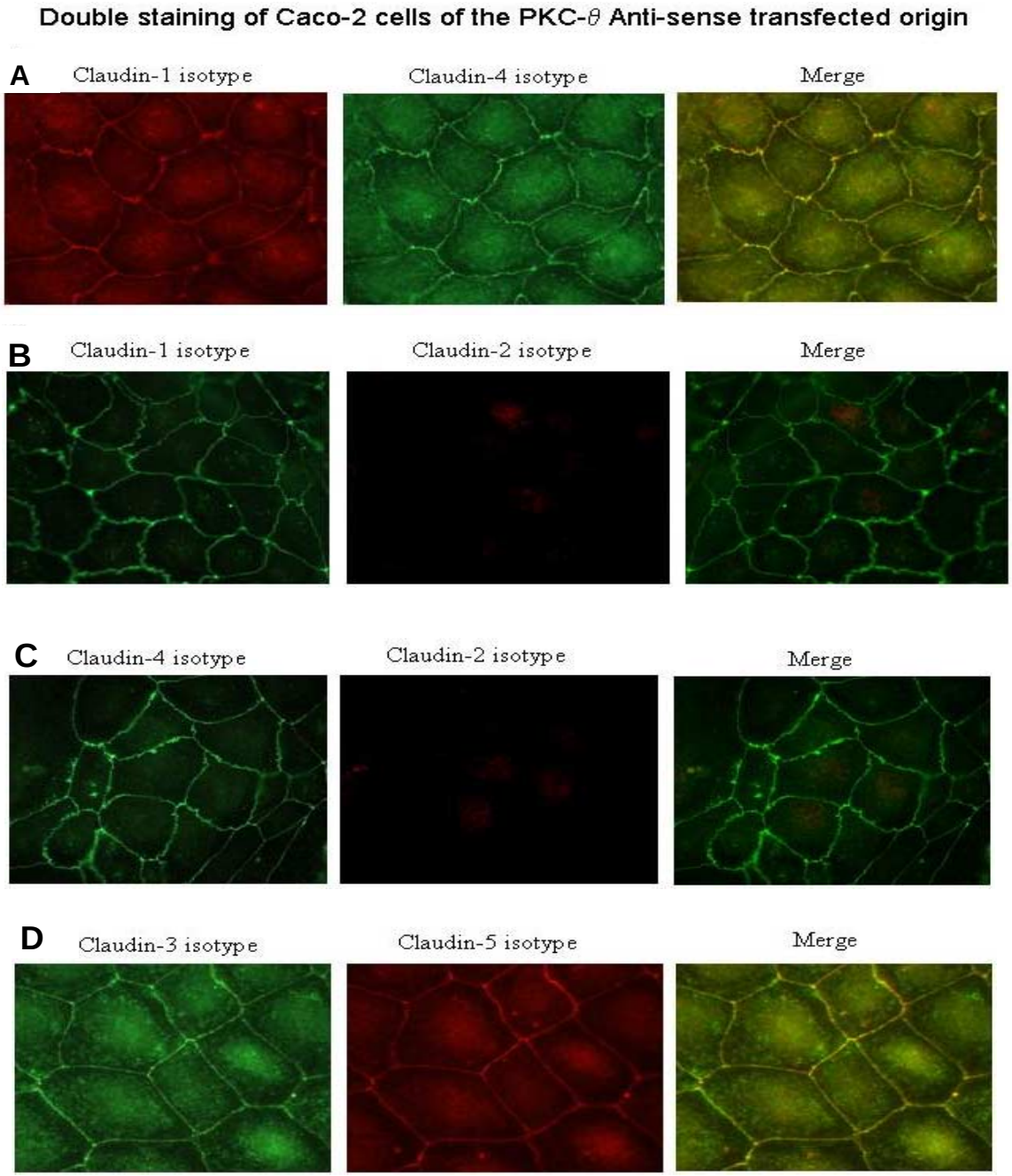

Figures 4A (top) and 4B (bottom).

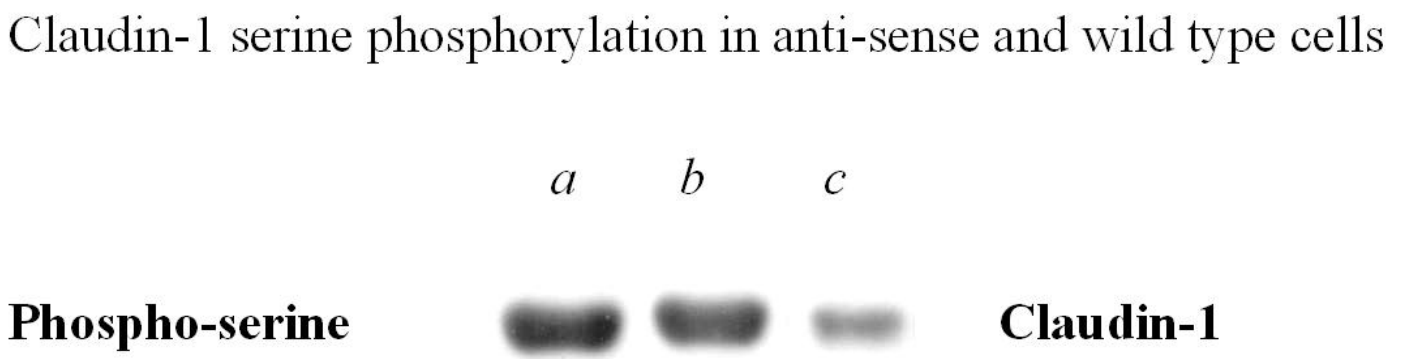

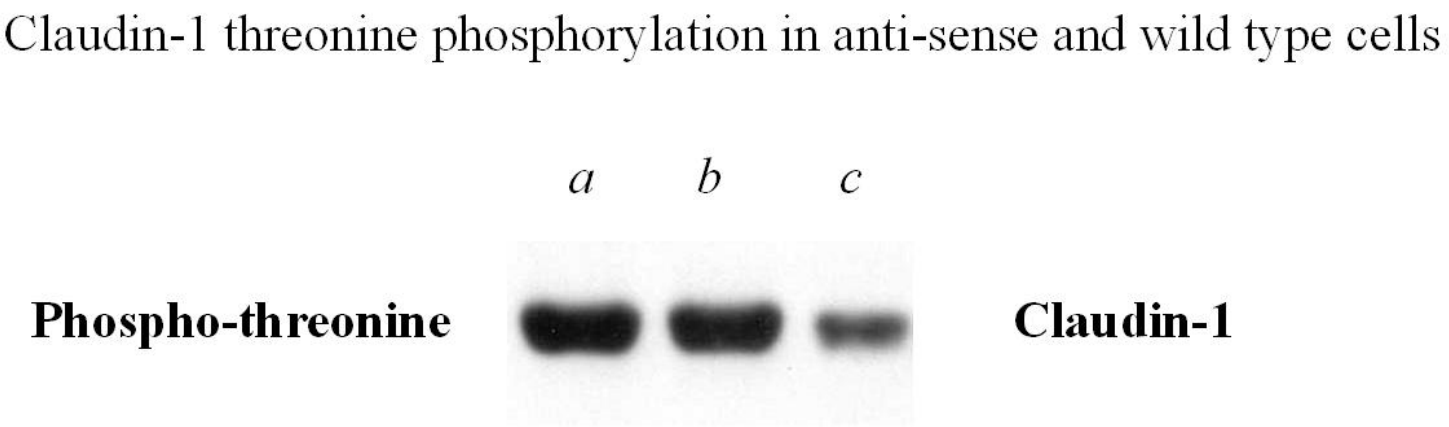

Figures 4C (top) and 4D (bottom).

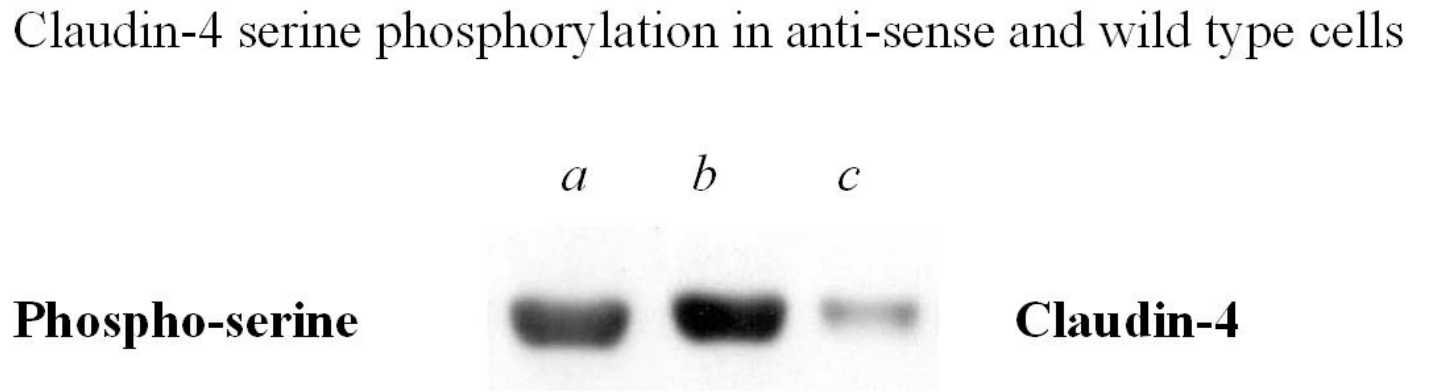

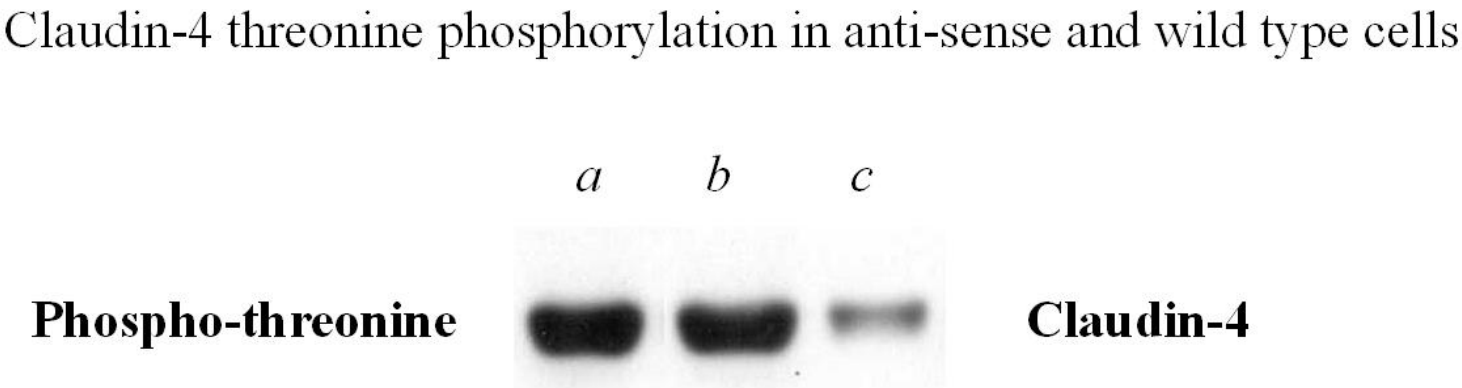

Figures 5A and 5B.

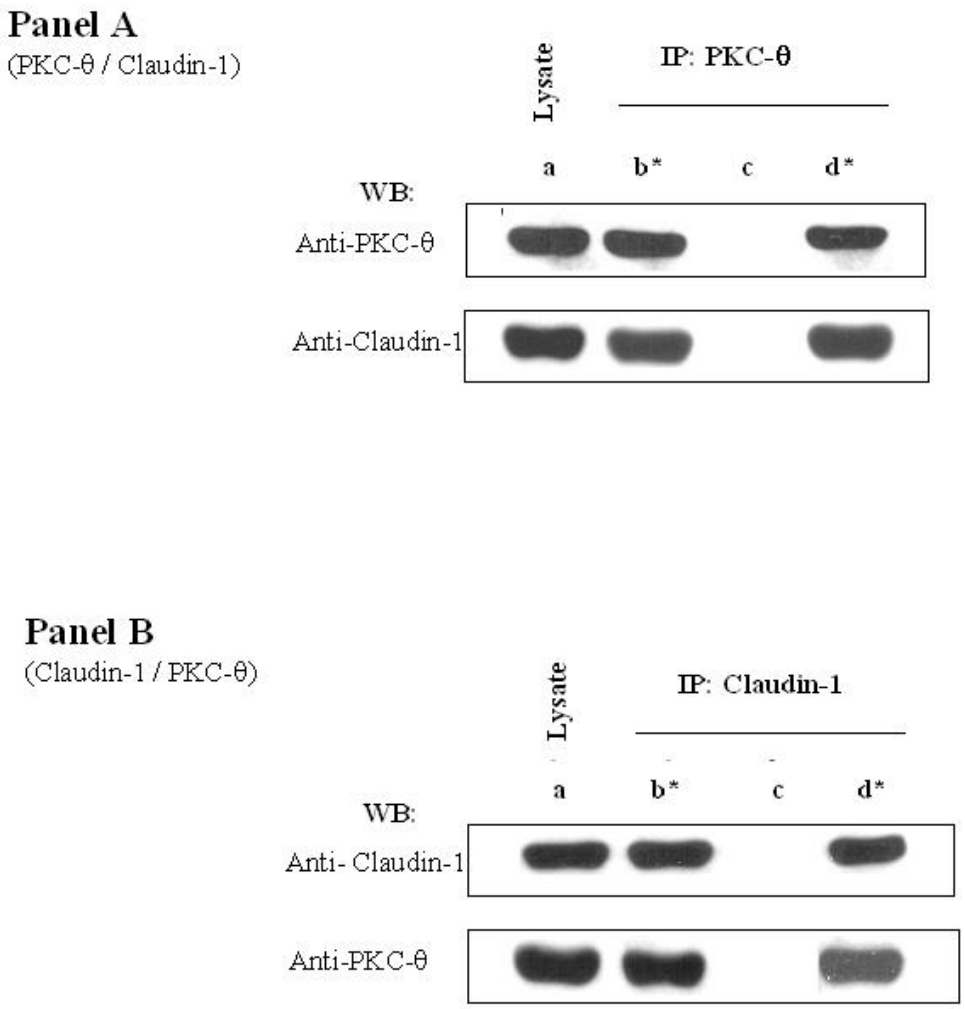

Figures 5C and 5D.

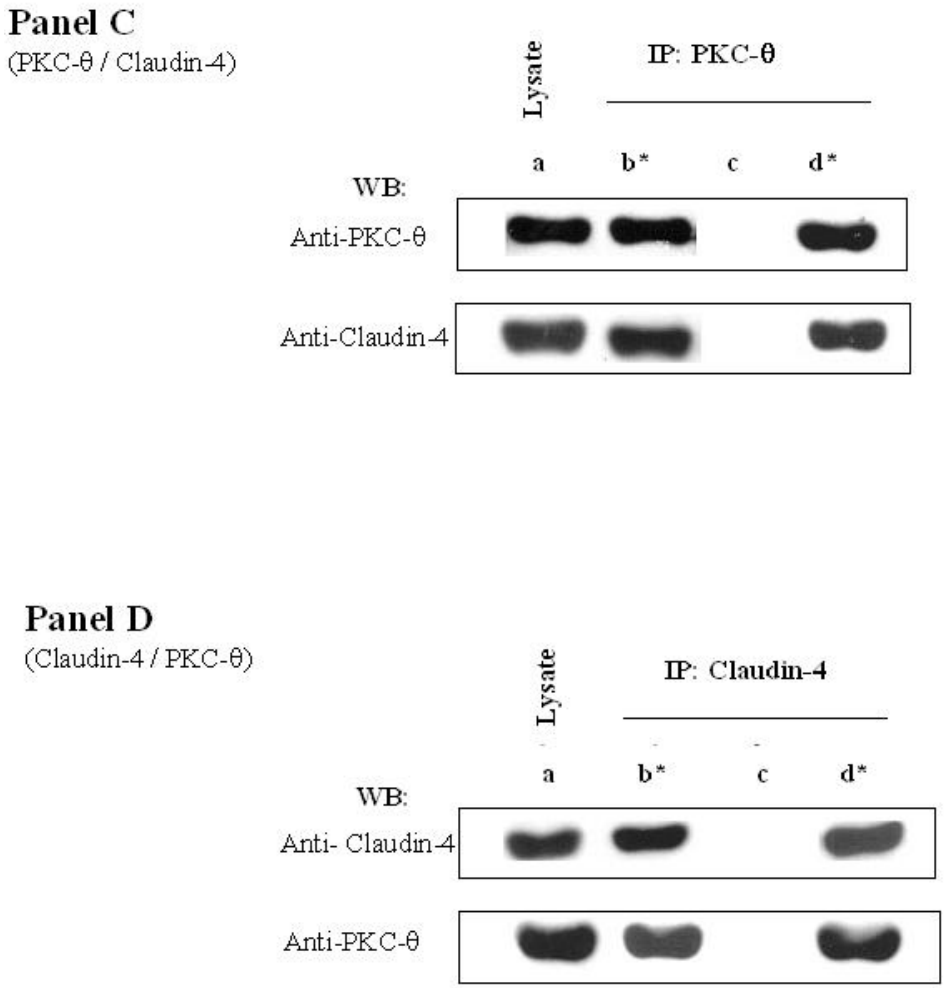

Figure 6A.

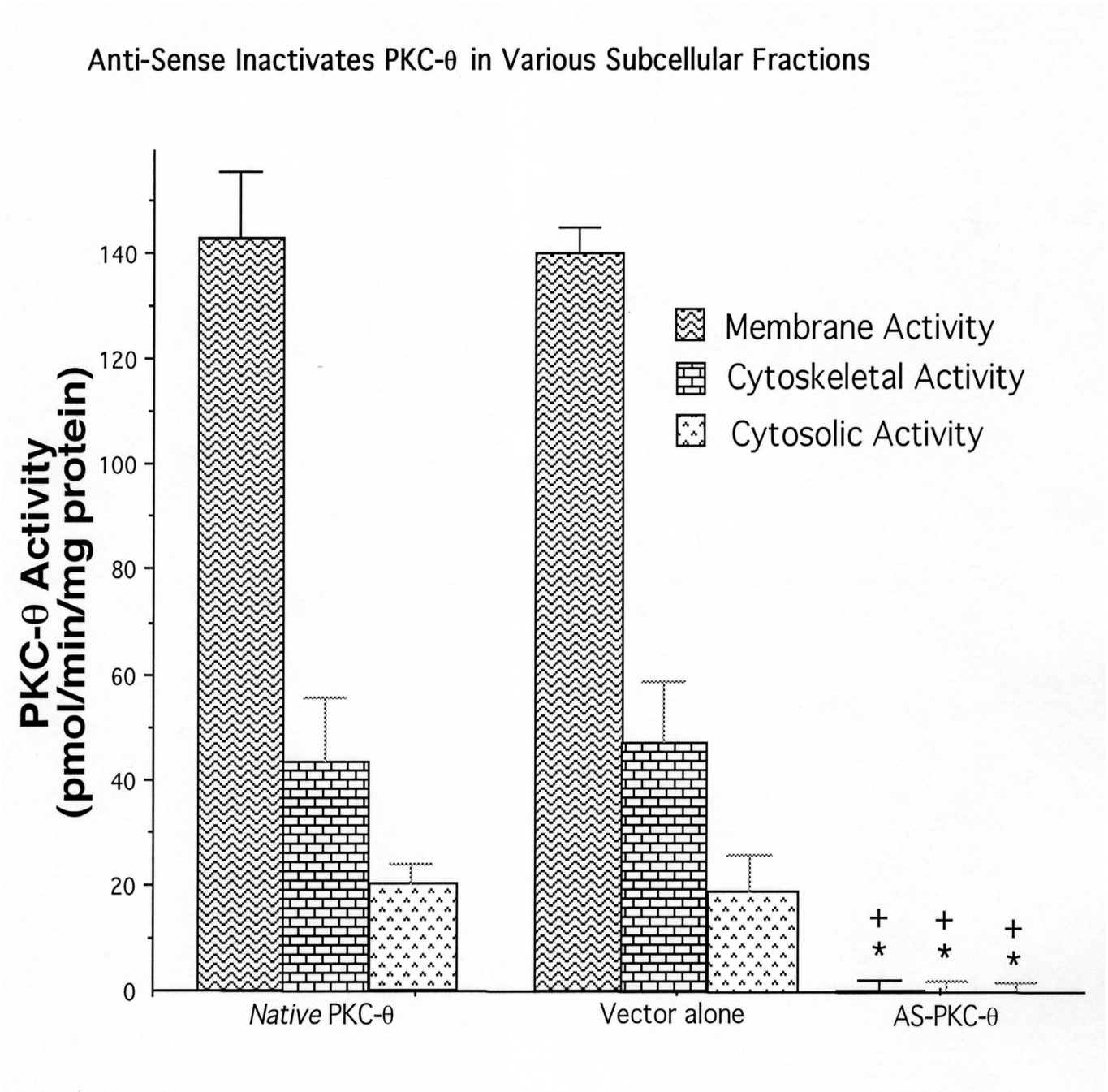

Figure 6B.

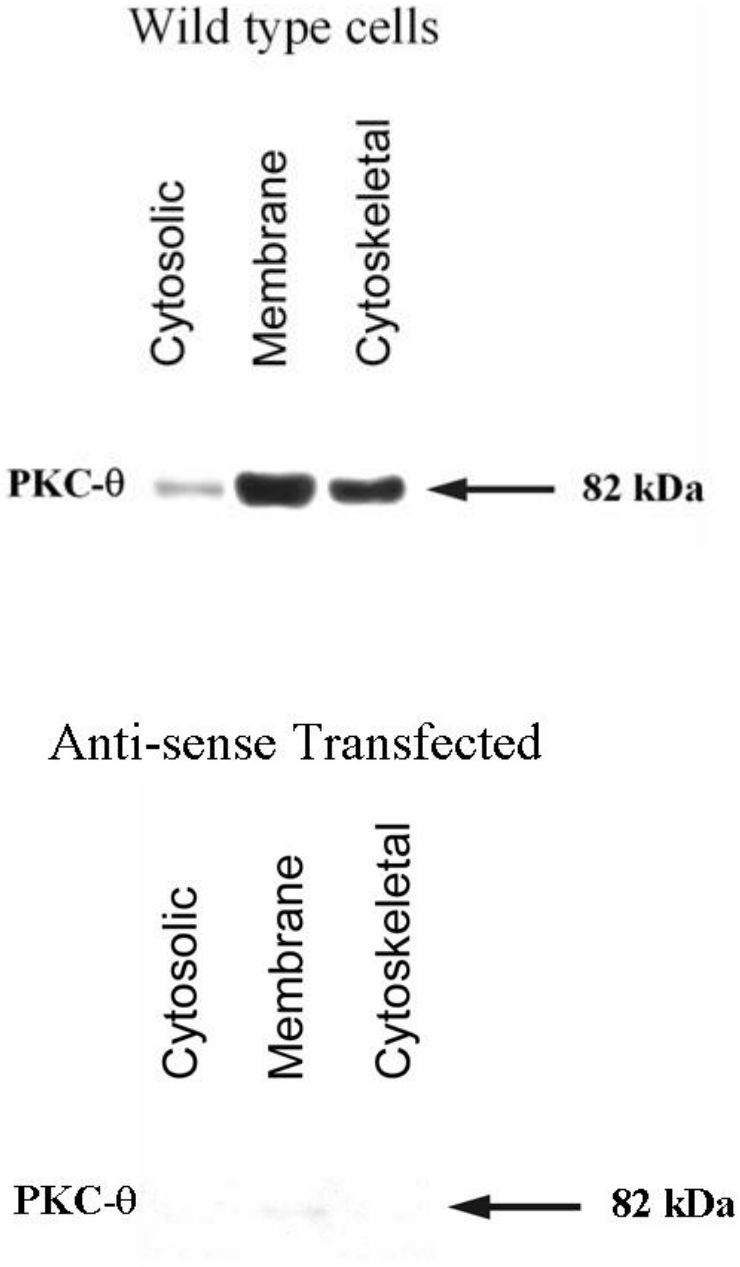

Figure 7.

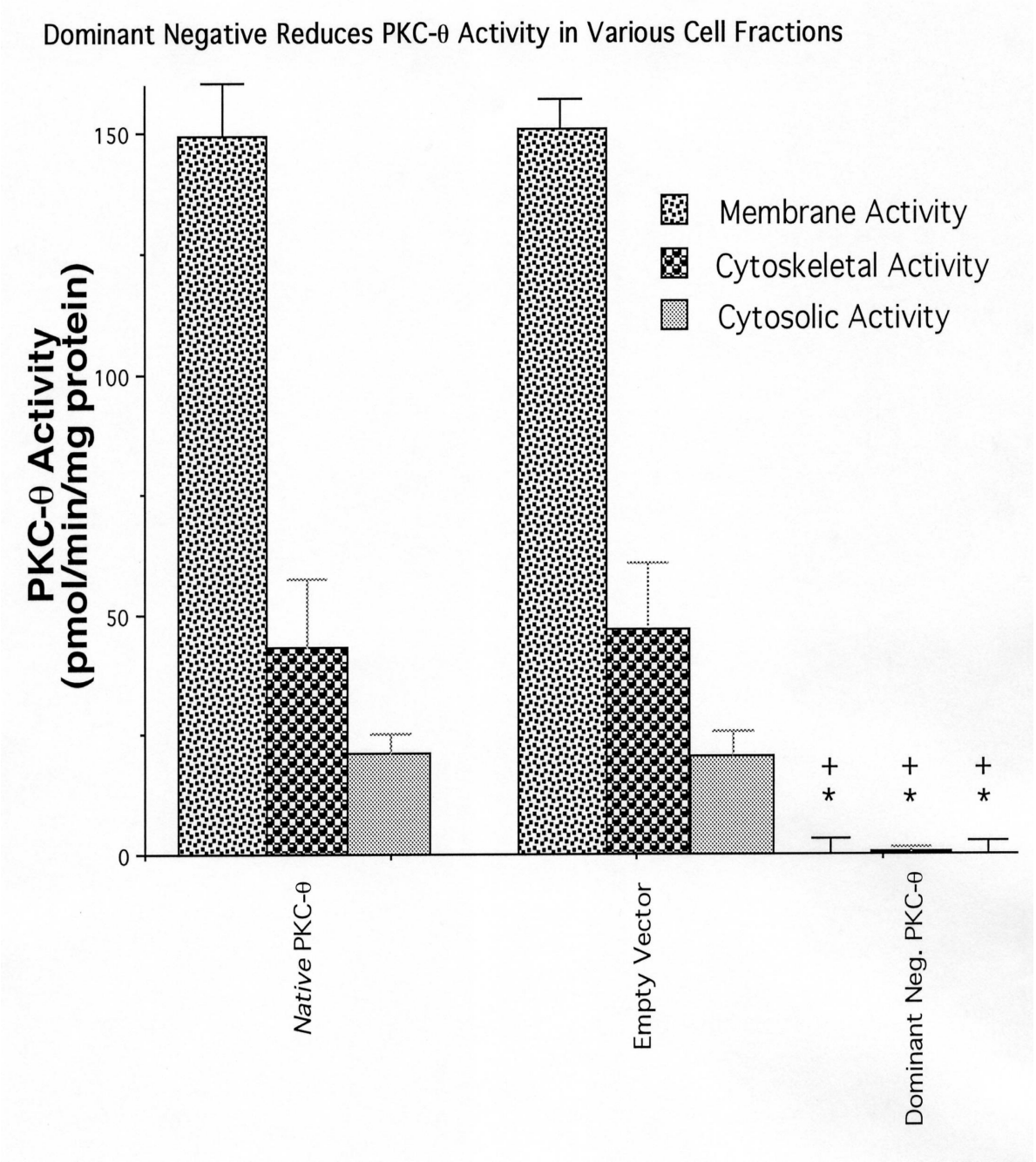

Figure 8A.

% Cells with normal Claudin-1 in dominant negative and wild type cells

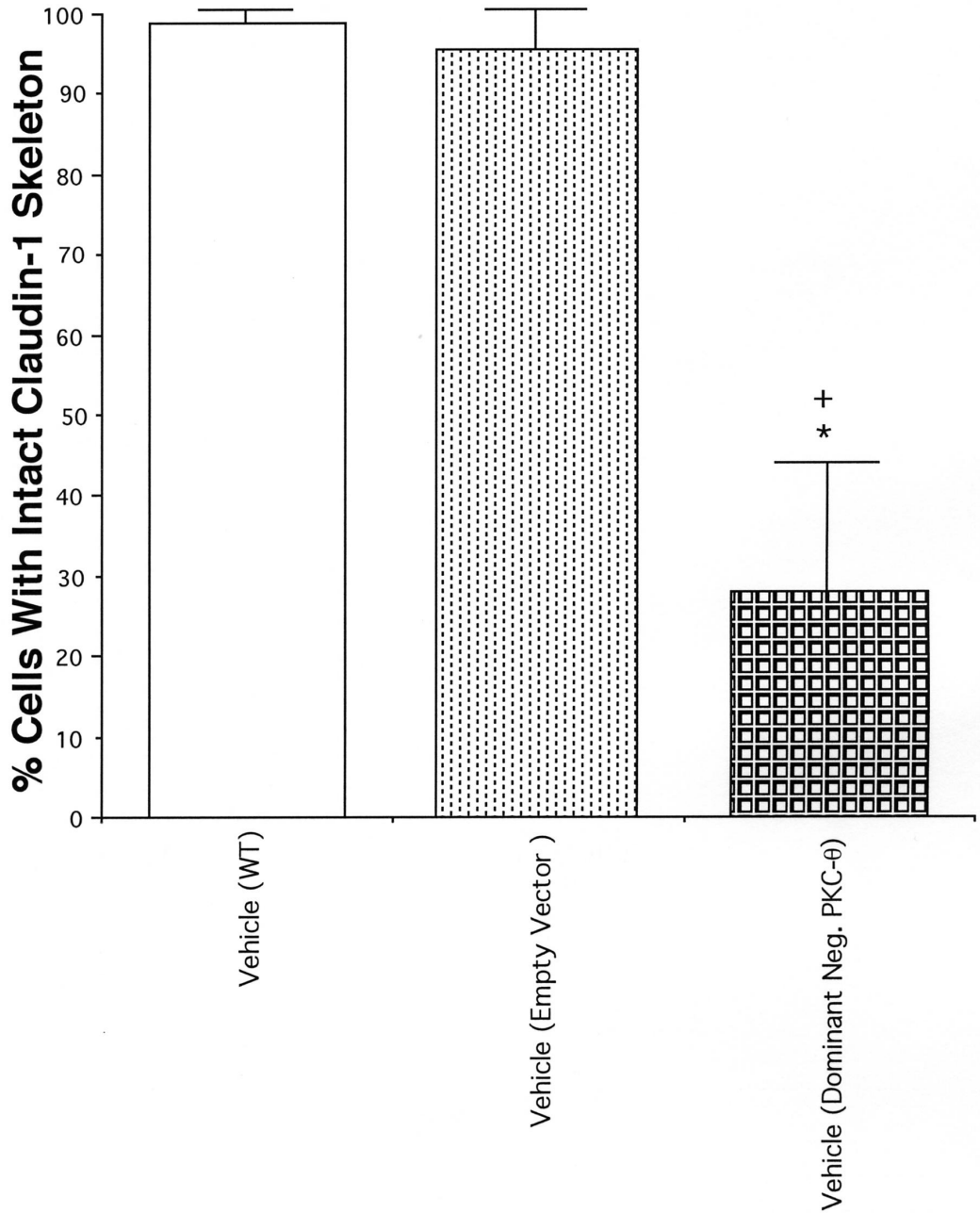

Figure 8B.

% Cells with normal Claudin-4 in dominant negative and wild type cells

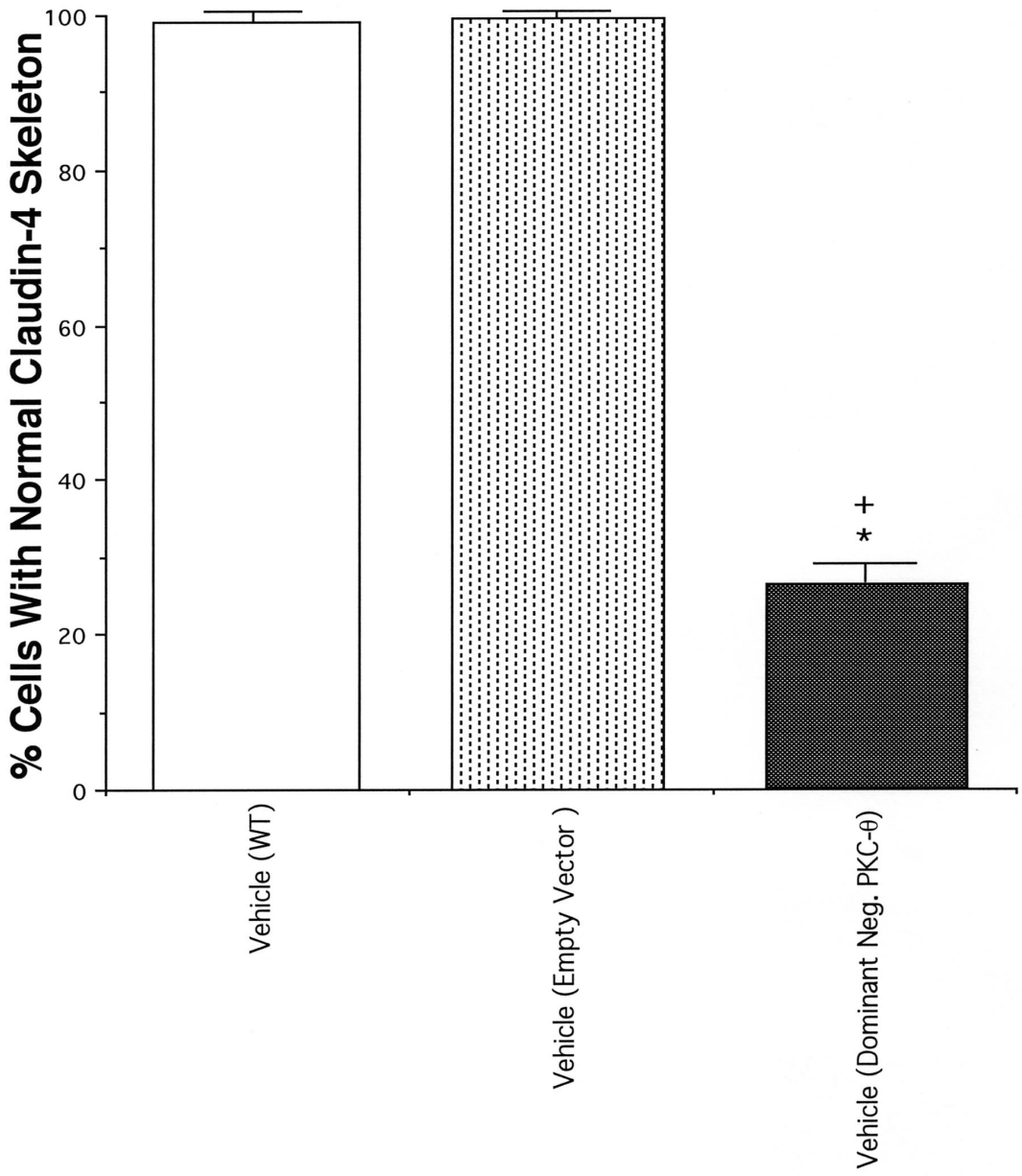

Figure 9.

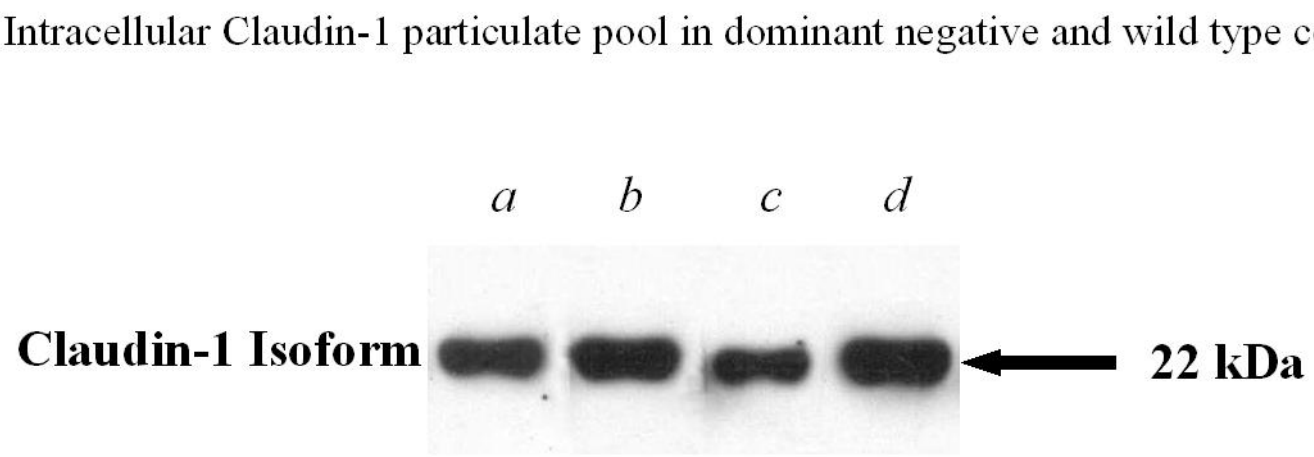

Figures 10A (top) and 10B (bottom).

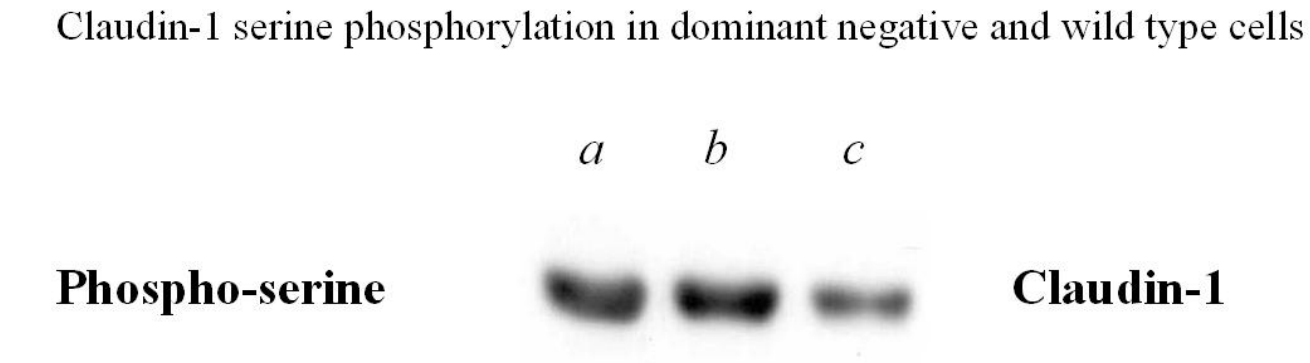

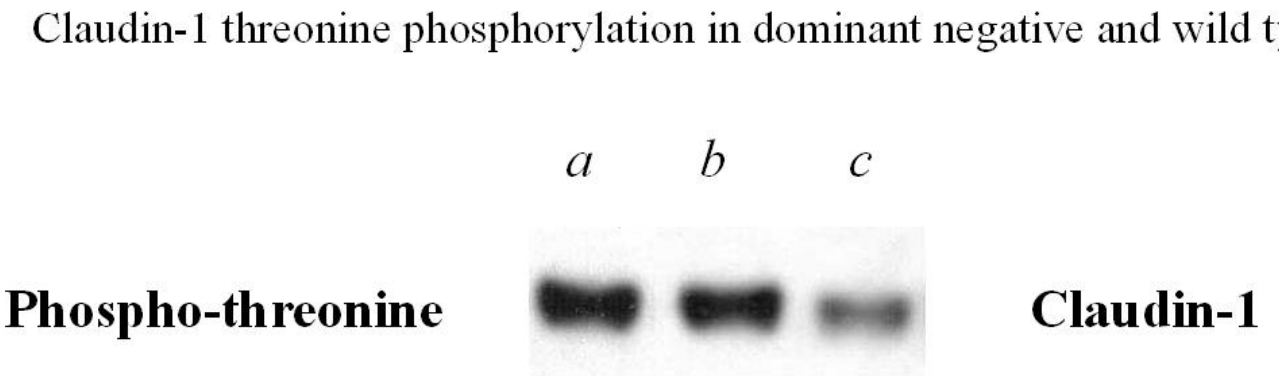

Figure 11A.

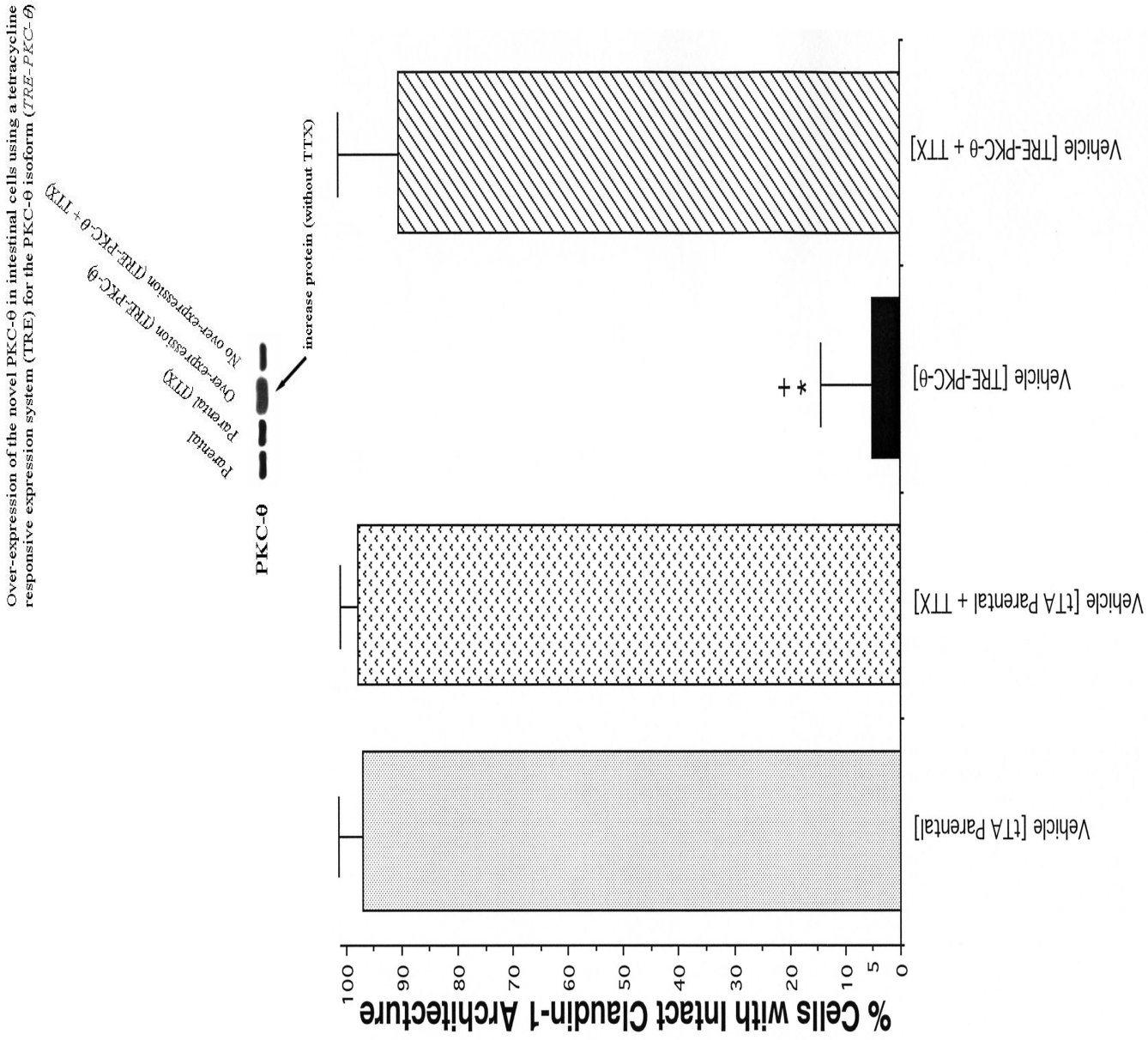

Figure 11B.

Representative images of Claudin-1 isotype architecture in over-expressing & parental monolayers

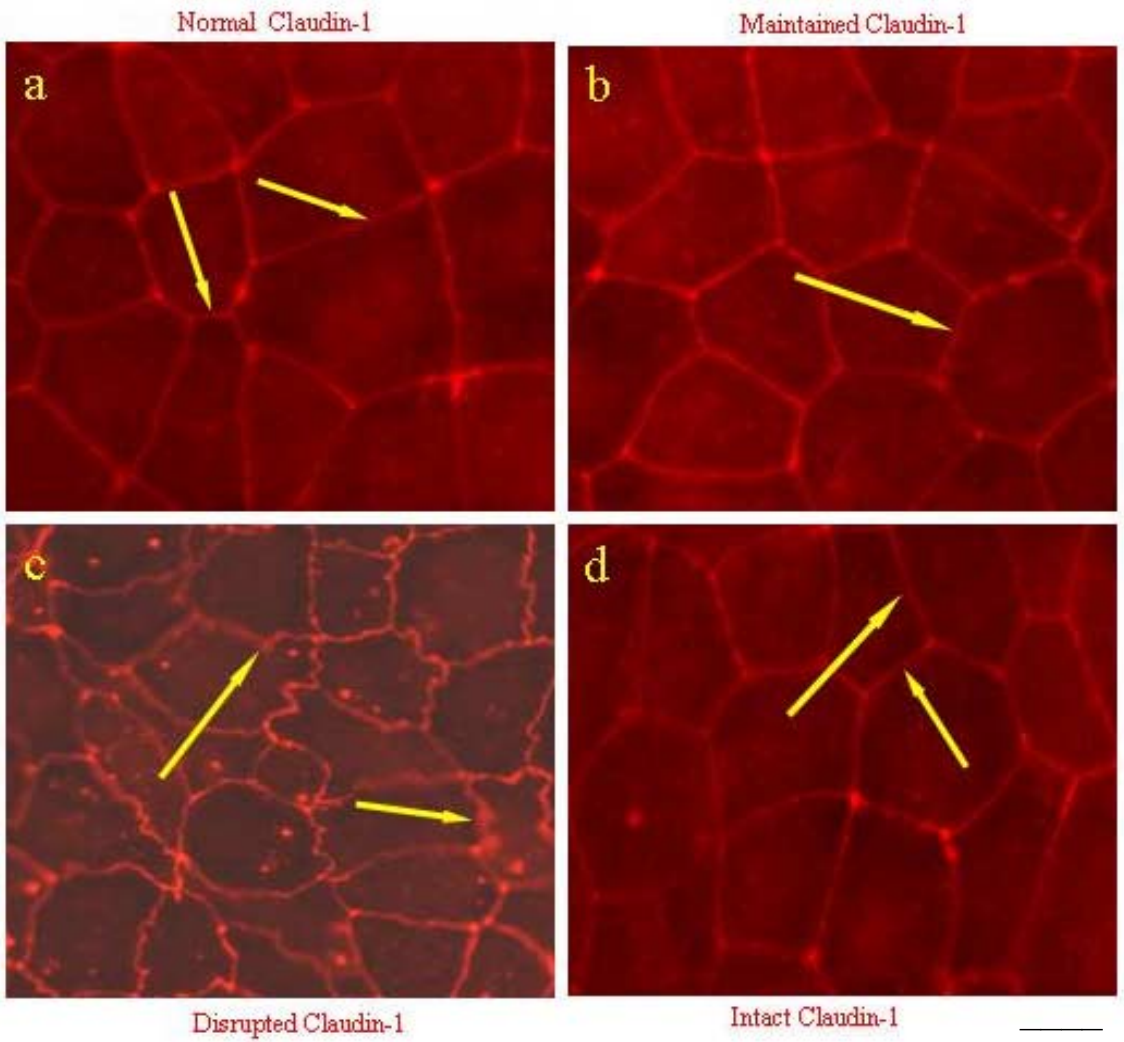

Figure 11B. Continued

Claudin-1 Architectural Details in Single Cells of Over-expressing and Parental Origin

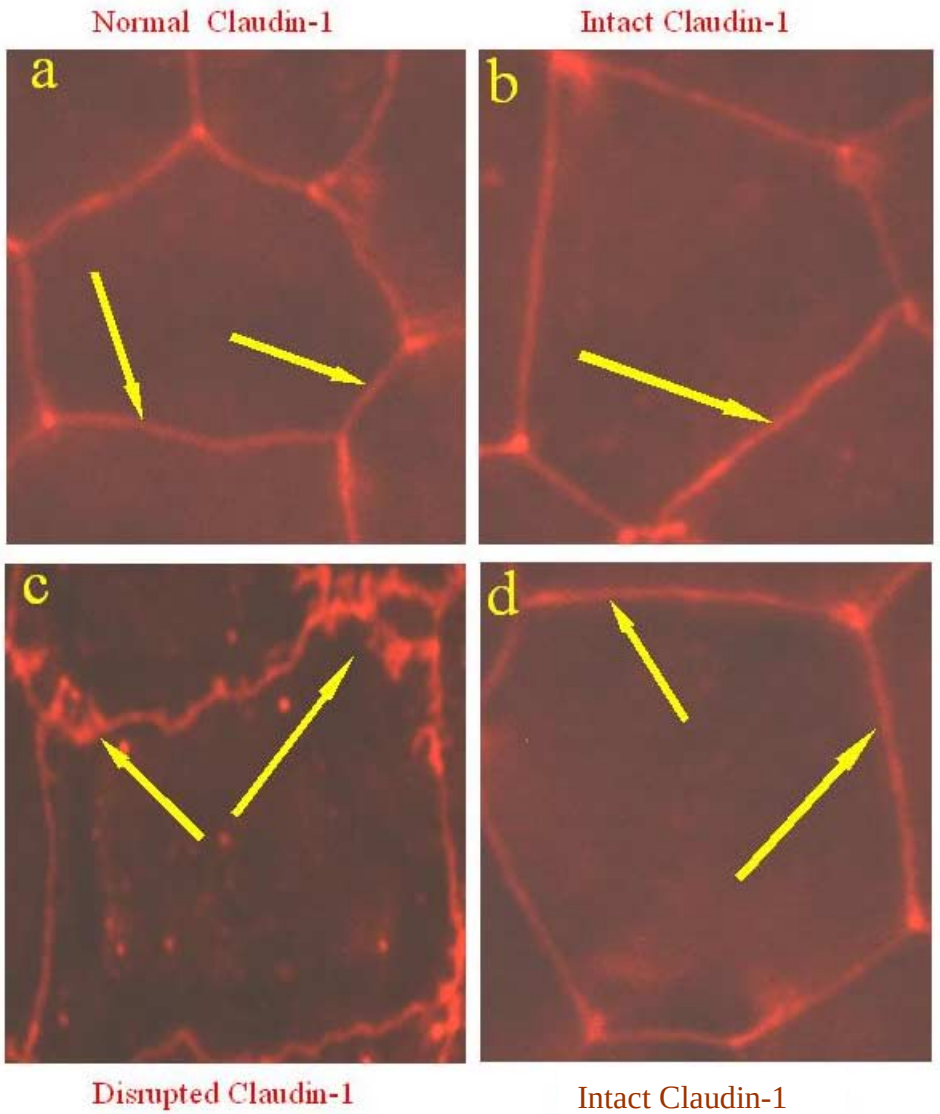

Figure 11C.

Representative Claudin-4 isotype cytoarchitecture in over-expressing and parental Monolayers

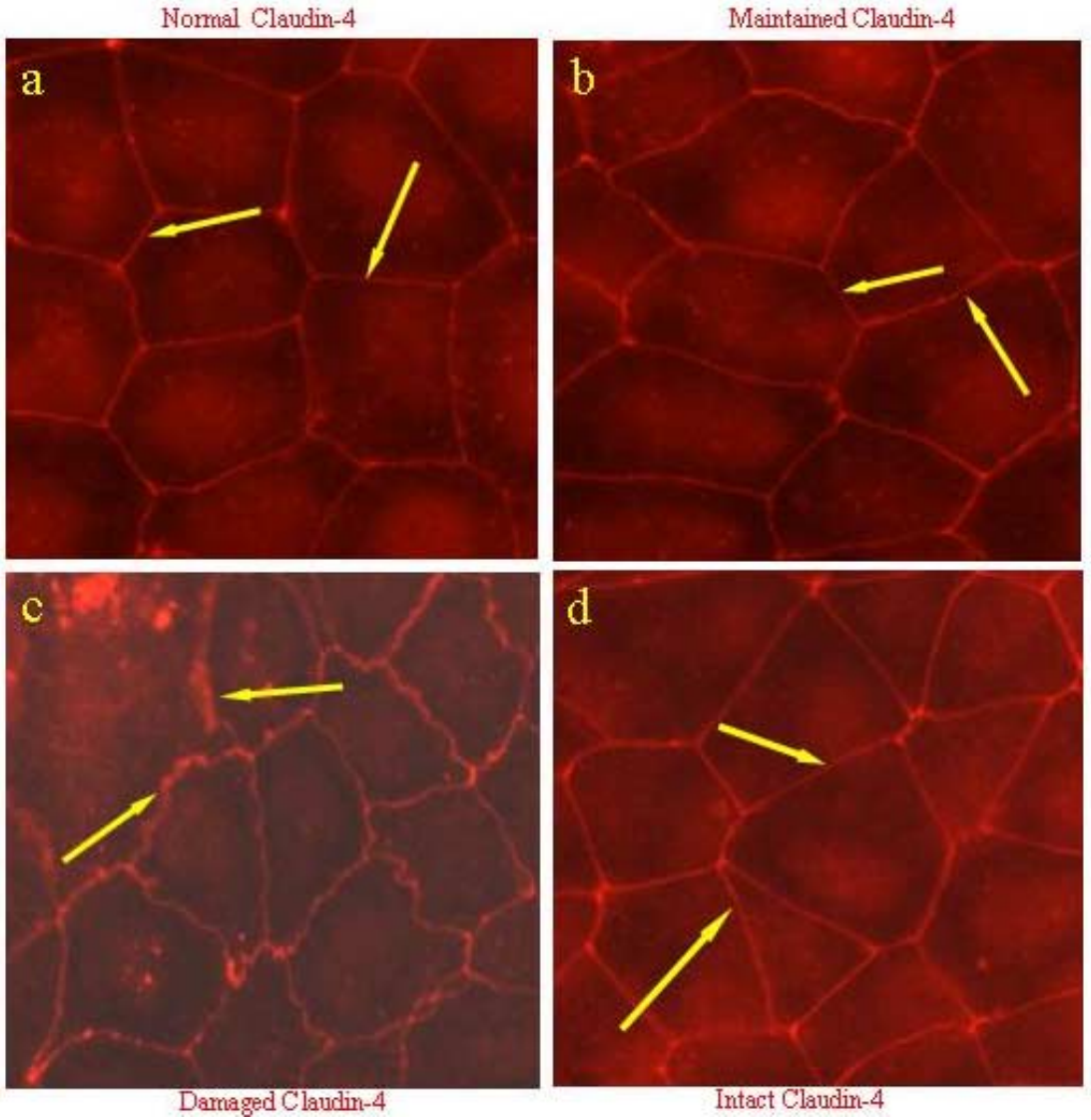

Figure 11C. Continued

Claudin-4 Architectural Details in Single Cells of Over-expressing and Parental Origin

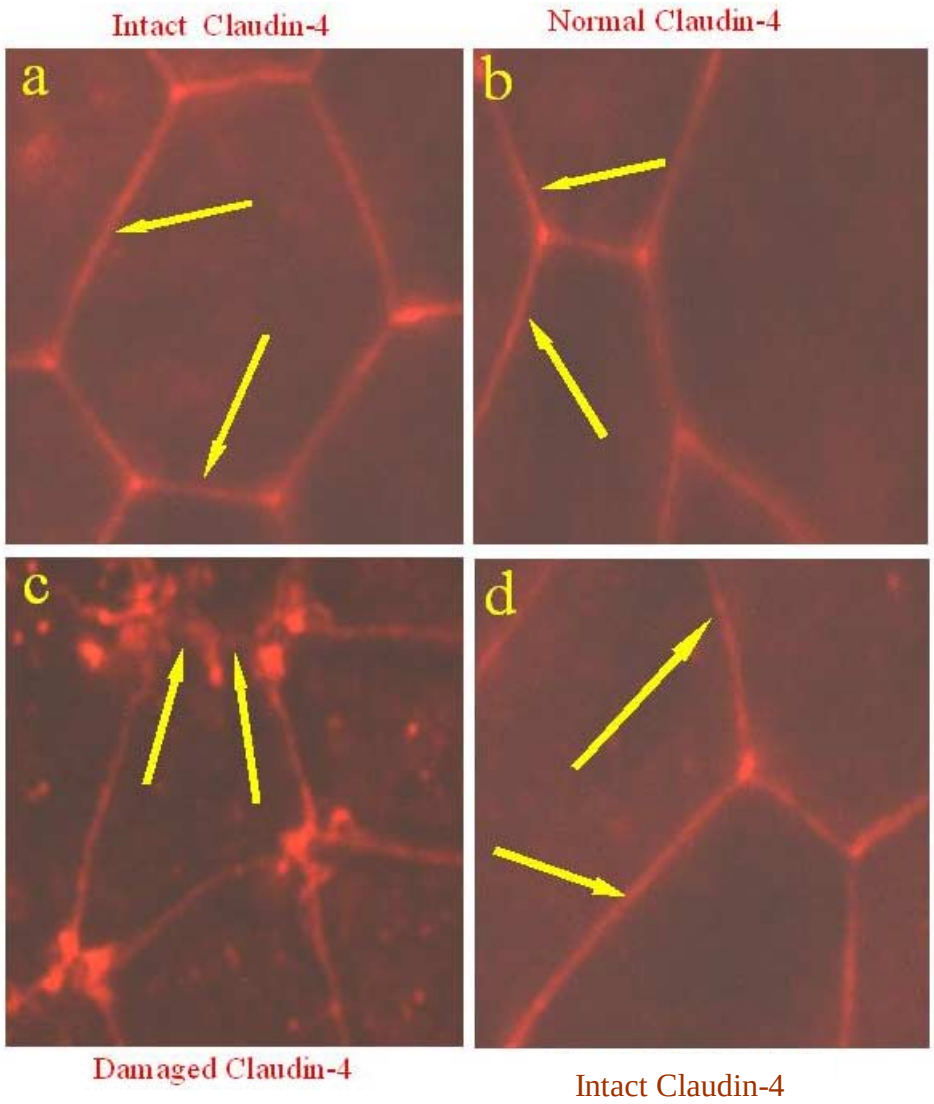

Figure 12.

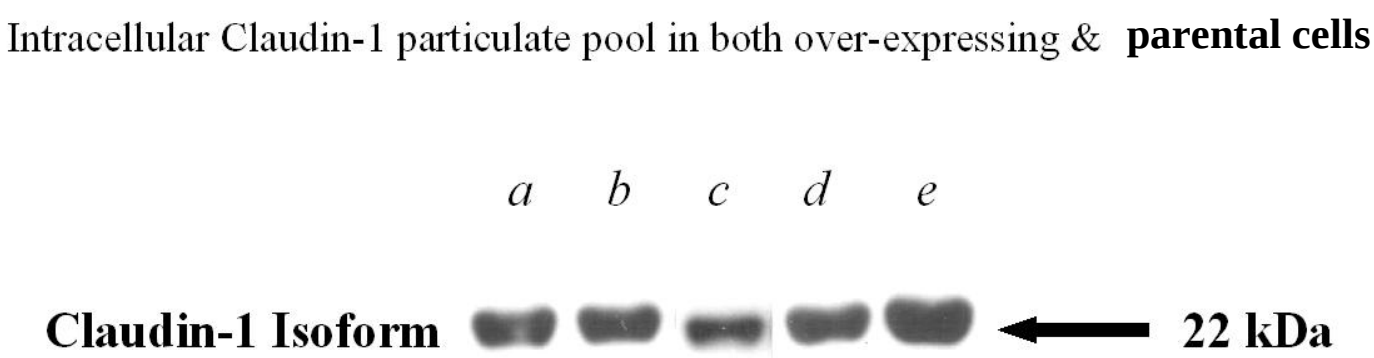

Figures 13A (top) and 13B (bottom).

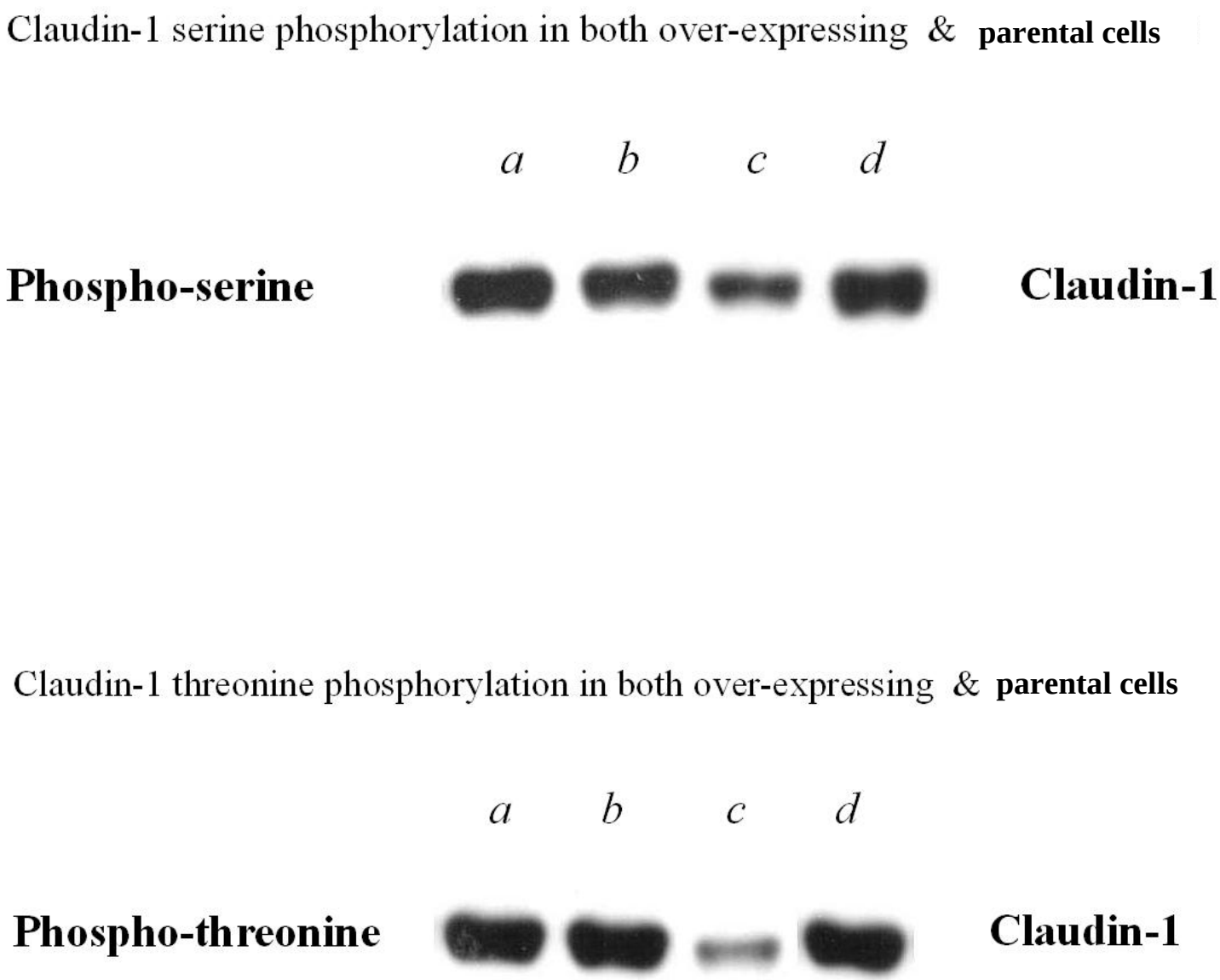

JPET Fast Forward. Published on March 10, 2005 as DOI: 10.1124/jpet.105.083428
This article has not been copyedited and formatted. The final version may differ from this version.

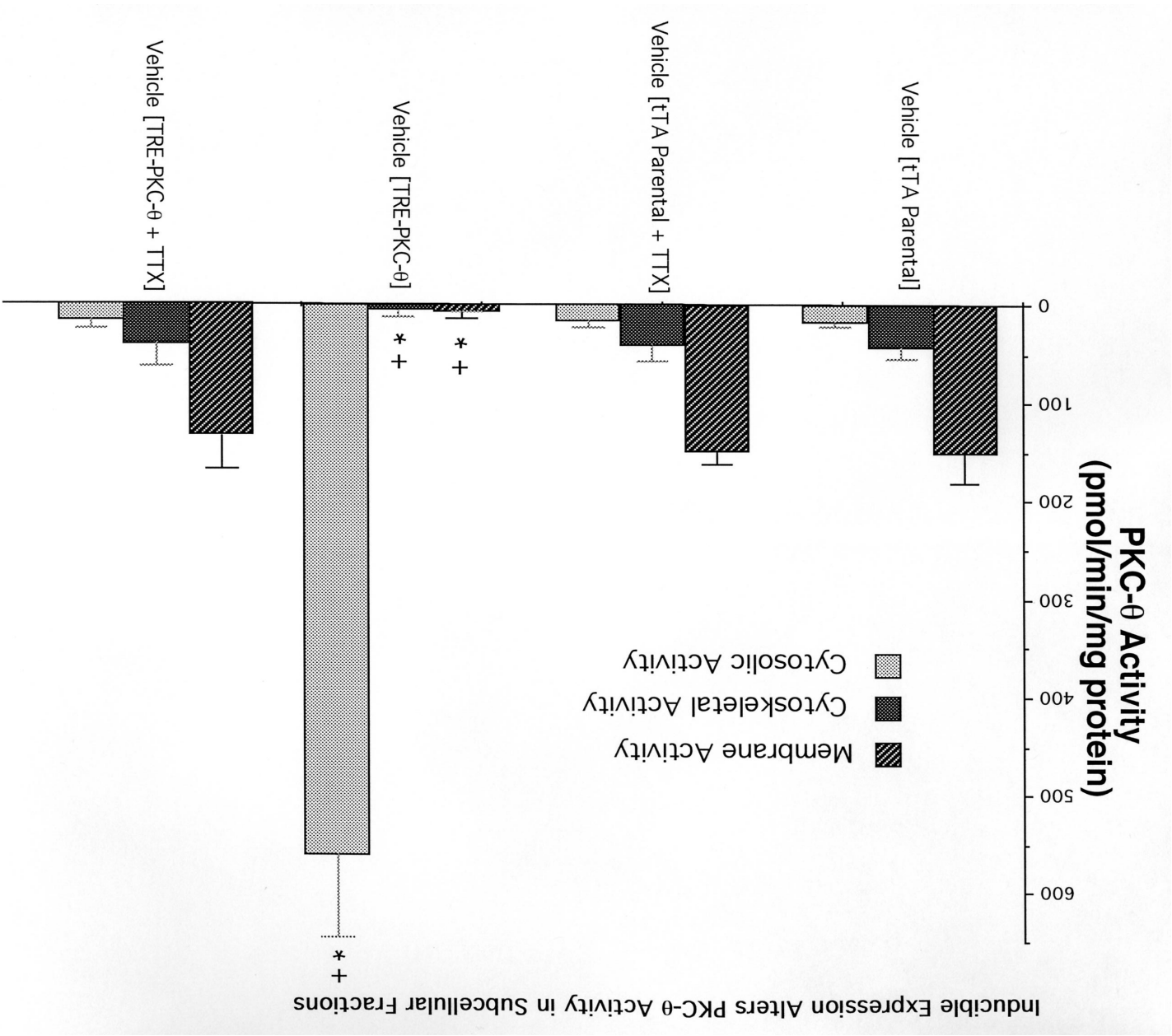

Figure 14.